

Score-driven threshold ice-age models: Benchmark models for long-run climate forecasts

Szabolcs Blazsek^a, Alvaro Escribano^{b,*}

^a School of Business, Universidad Francisco Marroquín, 01010, Guatemala City, Guatemala

^b Department of Economics, Universidad Carlos III de Madrid, 28903, Getafe, Spain

ARTICLE INFO

JEL classification:

C32
C38
C51
C52
C53
Q54

Keywords:

Climate change
Global ice volume
Atmospheric CO₂ level
Antarctic land surface temperature
Dynamic conditional score
Generalized autoregressive score
Score-driven ice-age models

ABSTRACT

Climate variables are known to be subject to abrupt changes when some threshold levels are surpassed. We use data for the last 798,000 years on global ice volume (Ice), atmospheric carbon dioxide level (CO₂), and Antarctic land surface temperature (Temp) to model and measure those long-run nonlinear climate effects. The climate variables have very long and asymmetric cycles, created by periods of upward trends, followed by periods of downward trends driven by exogenous orbital variables. The exogenous orbital variables considered by the Milankovitch cycles are eccentricity of Earth's orbit, obliquity, and precession of the equinox. We show that our new score-driven threshold ice-age models improve the statistical inference and forecasting performance of competing ice-age models from the literature. The drawback of using our 1000-year frequency observations, is that we cannot measure the nonlinear climate effects of humanity created during the last 250 years, which are known to have generated abrupt structural changes in the Earth's climate, due to unprecedented high levels of CO₂ and Temp, and low levels of Ice volume. On the other hand, the advantage of using low-frequency data is that they allow us to obtain long-run forecasts on what would have occurred if humanity had not burned fossil fuels since the start of the Industrial Revolution. These long-run forecasts can serve as benchmarks for the long-run evaluation of the impact of humanity on climate variables. Without the impact of humanity on climate, we predict the existence of turning points in the evolution of the three climate variables for the next 5,000 years: an upward trend in global ice volume, and downward trends in atmospheric CO₂ level and Antarctic land surface temperature.

1. Introduction

Climate change is the most important global issue on Earth. Compared to the end of the 19th century, the global surface temperature for the end of the 21st century is very likely to rise by 1.0 to 1.8 degrees Celsius (°C) under the “very low greenhouse gas emissions scenario”, by 2.1 to 3.5 °C for the “intermediate scenario”, and by 3.3 to 5.7 °C under the worst-case scenario, “very high greenhouse gas emissions scenario” (Intergovernmental Panel on Climate Change, 2021). The latter scenario implies dramatic consequences on nature and wildlife in terrestrial, wetland, and ocean ecosystems, and on humanity with respect to food and water security, migration, health, higher risk of conflict worldwide, reduction of global economic product, and a possible collapse of the current societal organization. Climate change is due to exogenous orbital variables during the history of Earth, and partly the influence of humanity during the most recent 10,000 to 15,000 years.

First, during the 4.5 billion-year history of Earth, climate change was driven by orbital variables which influenced global ice volume,

atmospheric carbon dioxide (CO₂) level, and land surface temperature. The atmospheric CO₂ level and land surface temperature are related to melting glaciers and sea ice. Hence, we name the climate-econometric models of those variables as ice-age models, in accordance with the work of Castle and Hendry (2020). The main orbital variables which drive Earth's climate are: (i) changes in the non-circularity of Earth's orbit with a period of 100,000 years, (ii) changes in the tilt of Earth's rotational axis relative to the ecliptic with a period of 41,000 years, and (iii) circular rotation of the rotational axis itself, which changes the season at which Earth's orbit is nearest to the Sun, with a period that is between 19,000 to 23,000 years. The cycles of those variables (i.e., the Milankovitch cycles) are the most important orbital variables which influence Earth's climate, and we use them as strictly exogenous explanatory variables in our climate-econometric models.

Second, the influence of humanity on Earth's climate started approximately 10,000 to 15,000 years ago, by commencing agricultural activities such as cultivating plants and livestock (Ruddiman, 2005).

* Correspondence to: Department of Economics, Universidad Carlos III de Madrid, Calle Madrid 126, Getafe (Madrid), 28903, Spain.

E-mail addresses: sblazsek@ufm.edu (S. Blazsek), alvaroe@eco.uc3m.es (A. Escribano).

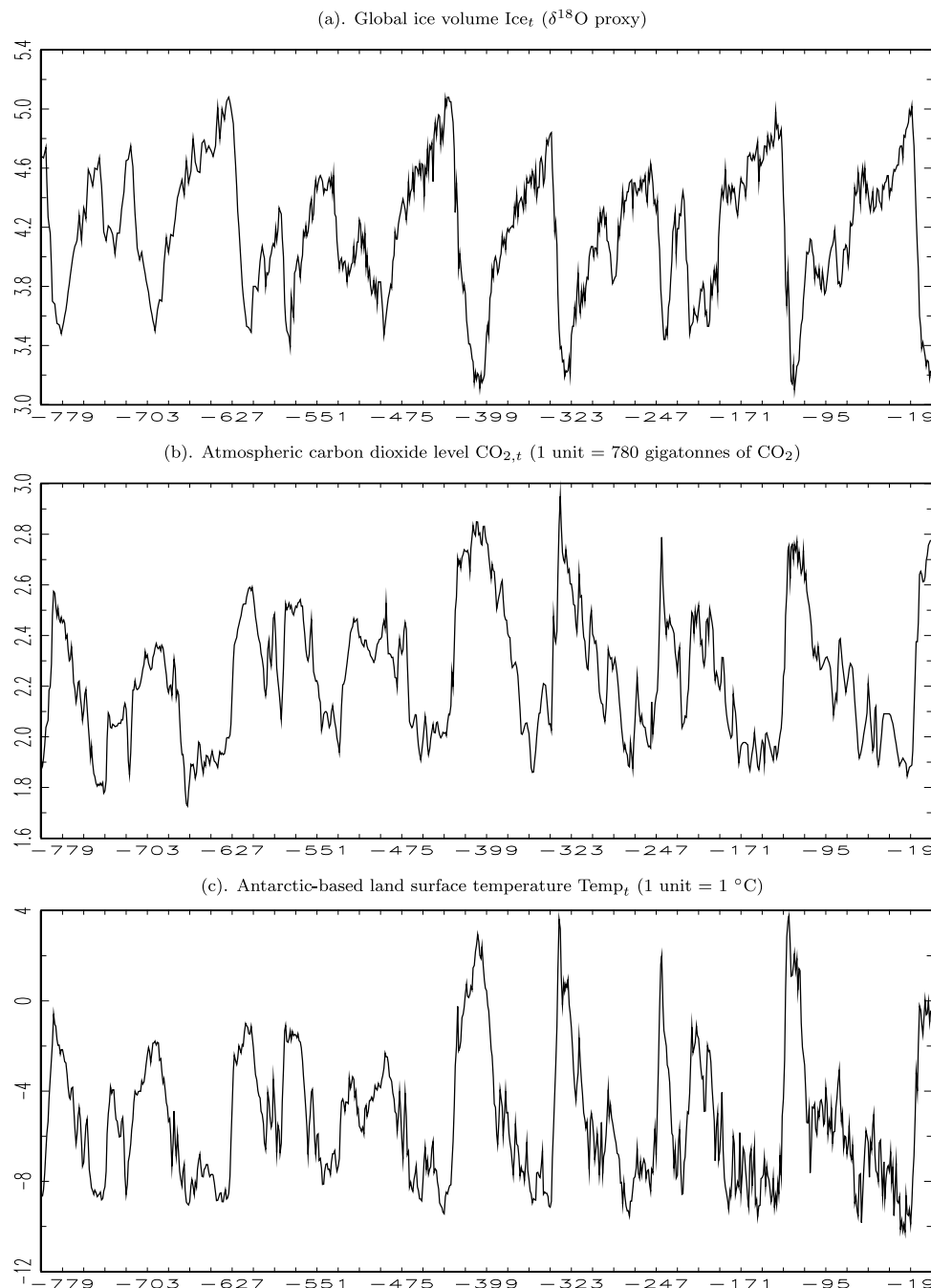


Fig. 1. Evolution of Ice_t , $CO_{2,t}$, and $Temp_t$ from 798,000 years ago to 1000 years ago.
Source: [Castle and Hendry \(2020\)](#).

That influence significantly increased after the Industrial Revolution (from 1769 to 1840, approximately), and it has further increased with an accelerating growth rate since then. Earth's population rose from 1 billion in 1800 to 8 billion in 2022, which was associated with a significant global-scale economic expansion. One of the consequences is rising global greenhouse gas emissions (GHGs).

In the recent work of [Blazsek and Escribano \(2022\)](#), the score-driven ice-age model is introduced, and it is shown that the statistical performance of the score-driven ice-age model is superior to the statistical performance of the ice-age model of [Castle and Hendry \(2020\)](#). Moreover, [Blazsek and Escribano \(2022\)](#) also show that the forecasting performances of both models are similar and not very effective for the climate variables for the last 10,000 to 15,000 years when humanity influenced Earth's climate. The present paper is motivated by this issue,

and we introduce the score-driven threshold ice-age model to improve forecasting performances.

We use the same data for climate and orbital variables for the last 798,000-year period as [Castle and Hendry \(2020\)](#) and [Blazsek and Escribano \(2022\)](#), and we forecast global ice volume, atmospheric CO_2 , and Antarctic land surface temperature for the last 100,000 years of the sample and the forthcoming 5000 years. We use 1,000-year frequency observations, which do not allow the measurement of climate effects of humanity for the last 250 years when a new regime started in Earth's climate with unprecedented high levels of $CO_{2,t}$ and $Temp_t$, and unprecedented low levels of Ice_t .

First, we introduce the score-driven Markov-switching (MS) ice-age model, and we provide evidence of structural changes in the climate, indicating periods of sharply increasing $CO_{2,t}$ and $Temp_t$. Motivated

by this, by using Ward's linkage clustering method (Ward, 1963), we define dummy variables which indicate subperiods in Earth's climate, and we introduce the score-driven threshold ice-age model. The results support the use of the threshold ice-age models, since the forecasting performances of the models of Castle and Hendry (2020) and Blazsek and Escribano (2022) for the last 100,000 years are improved. Our in-sample forecasting results, compared to the corresponding results of the aforementioned authors are impressive, motivating the use of the new score-driven threshold ice-age models. Finally, we provide out-of-sample forecasts of the climate variables for the following 5000 years, and we show a turning point for the climate variables: an increasing global ice volume Ice_t , a decreasing atmospheric $CO_{2,t}$ volume, and a decreasing Antarctic land surface temperature $Temp_t$ are predicted for the forthcoming period. Those forecasts can be interpreted as benchmarks, which would have occurred if humanity had not burned any fossil fuels since the Industrial Revolution.

The remainder of this paper is organized as follows: Section 2 describes the climate and orbital data. Section 3 presents the econometric methods and the empirical results. Section 4 concludes.

2. Data

All data in this paper are from Jennifer L. Castle and David F. Hendry (Castle and Hendry, 2020). In this section, we provide a description of the dependent and explanatory variables.

The dependent variables are global ice volume Ice_t , atmospheric $CO_{2,t}$ volume, and Antarctic land surface temperature $Temp_t$, which are observed for the period of 798,000 years ago to 1000 years ago with a 1,000-year observation frequency. The data source of global ice volume Ice_t is the work of Lisiecki and Raymo (2005), in which time series of the $\delta^{18}O$, obtained from calcium carbonate ($CaCO_3$) shells of foraminifera, are used to approximate temperature. Those authors use benthic records of foraminifera from seafloor sediment, which were collected at 57 globally distributed sites. Those sites are well-distributed in latitude, longitude, and depth in the Atlantic, Pacific, and Indian Oceans. The data source of atmospheric $CO_{2,t}$ is the work of Lüthi et al. (2008), in which changes in past atmospheric CO_2 concentrations are determined by measuring the composition of air trapped in ice cores from Antarctica. Within the European Project for Ice Coring in Antarctica (EPICA), two deep ice cores have been drilled at the Kohnen Station and the Concordia Station (Dome C). The drillings were stopped at or a few meters above bedrock at a depth of 2,774 meters and 3,270 m, respectively. The data source of Antarctic land surface temperature $Temp_t$ is the work of Jouzel et al. (2007), in which temperature data were obtained within the EPICA at the Concordia Station (Dome C), by using deuterium δD_{ice} measurements from the surface down to 3,259.7 m.

The exogenous explanatory variables are eccentricity of Earth's orbit Ec_t , obliquity of Earth's rotational axis relative to the ecliptic Ob_t , and precession of the equinox Pr_t . We obtained data for the period of 798,000 years ago to 100,000 years in the future (from the present) with a 1,000-year observation frequency. Nevertheless, for the out-of-sample predictions of this paper, we focus on the data for the forthcoming 5000 years from the future data. The sources of those data are the works of Paillard et al. (1996) and Castle and Hendry (2020). Additional explanatory variables, which are exogenous to humanity are omitted from the econometric models of this paper. For example, the following variables are omitted: (i) the variations in the Sun's radiation output, (ii) volcanic eruption particles in the atmosphere and ice cover, and (iii) changes in the magnetic poles. For further discussion on why these variables are omitted, see the Appendix in the work of Blazsek and Escribano (2022).

In Table 1, the dependent and explanatory variables for the historical period are presented. The table shows the definitions of variables, observation period, units of measurement, data sources, and some

descriptive statistics for each variable. Due to the 1,000-year observation frequency, we cannot measure the effects of humanity on Earth's climate for the last decades, or predict climate data for the forthcoming decades. Hence, we cannot comment on the results of the Intergovernmental Panel on Climate Change (2021), and we are not able to measure the impact of humanity compared to the climate impact of the Milankovitch cycles since the Industrial Revolution. Therefore, the forecasts of future values of the climate variables reported in this paper can be interpreted as benchmarks, which would have occurred if the humanity had not burned any fossil fuels during the last 250 years.

In Figs. 1 and 2, the evolution of the dependent and explanatory variables, respectively, are presented. According to Figs. 1(b) and 1(c), atmospheric $CO_{2,t}$ and Antarctic land surface temperature $Temp_t$, respectively, remarkably are in unison. In Fig. 1(a), it can also be noticed that global ice volume Ice_t moves in the opposite direction from $CO_{2,t}$ and $Temp_t$, creating the ice-age and inter-glacial periods periodically. The cyclical evolution of the dependent variables, which is partly due to the three main interacting orbital changes over time affecting solar radiation, is clearly observed in Figs. 1 and 2.

In Fig. 1, a significant impact of the Milankovitch cycles on Earth's temperature is observed for the last 21,000 years, when the Antarctic land surface temperature increased from the $-9.5177^\circ C$ of 21,000 years ago to the $-0.2174^\circ C$ of 11,000 years ago. That sharp increase is due to the Milankovitch cycles, because during that period of time humanity had little influence on Earth's climate. From 10,000 to 1000 years ago, when humanity influenced more Earth's climate, the Antarctic land surface temperature was at a relatively stable high level with a $-0.6060^\circ C$ average and a $0.4539^\circ C$ standard deviation. Hence, from the Antarctic land surface temperature time series we do not see direct evidence of the impact of humanity on climate for the period of the last 10,000 years. Our results can be used as benchmarks for researchers who use more frequently observed data for the last 250 years to predict climate variables, in order to separate the effects of orbital variables and humanity in their forecasts.

3. Climate-econometric models

3.1. Score-driven ice-age model

Score-driven time series models are introduced in the works of Creal et al. (2008) and Harvey and Chakravarty (2008). Those authors name the score-driven models generalized autoregressive score (GAS) and dynamic conditional score (DCS) models, respectively. Score-driven models are observation-driven time series models (Cox, 1981), in which the filters are updated using the scaled conditional score functions of the log-likelihood (LL) of the dependent variables. Score-driven models are estimated by using the maximum likelihood (ML) method (Harvey, 2013; Blasques et al., 2022).

Some of the statistical advantages of the score-driven models are the following. (i) The updating mechanisms of those models are generalizations of those of the classical time series models such as: ARMA (autoregressive moving average) (Box and Jenkins, 1970), GARCH (generalized autoregressive conditional heteroskedasticity) (Engle, 1982; Bollerslev, 1986), and VARMA (vector ARMA) (Tiao and Tsay, 1989). (ii) Score-driven models are robust to outliers and missing observations (Harvey, 2013; Blazsek and Escribano, 2016a,b, 2022; Ayala et al., 2022). (iii) A score-driven update locally reduces the Kullback–Leibler distance between the true and estimated values of the score-driven filter in every step, and only score-driven models have this property (Blasques et al., 2015). Thus, score-driven filters use an information-theoretically optimal updating mechanism. These advantages of the score-driven models motivate their application to climate data. We also note that the linear updating mechanisms of ARMA and VARMA, and the quadratic updating mechanism of GARCH are optimal from an information-theoretic perspective only if the data generating process

Table 1
Descriptive statistics.

(a) Dependent variables	Ice _{<i>t</i>}	CO _{2,t}	Temp _{<i>t</i>}
Variable	Ice volume	Atmospheric CO ₂	Antarctic-based land surface temperature
Data frequency	1,000 years	1,000 years	1,000 years
Measurement	Based on the δ ¹⁸ O proxy	1 unit = 780 gigatonnes of CO ₂	1 unit = 1 °C
Data source	Lisiecki and Raymo (2005)	Lüthi et al. (2008)	Jouzel et al. (2007)
Descriptive statistics for the dependent variables for the historical period:			
Start date	798,000 years ago	798,000 years ago	798,000 years ago
End date	1,000 years ago	1,000 years ago	1,000 years ago
Sample size	798	798	798
Minimum	3.1000	1.7269	-10.2530
Maximum	5.0800	2.9500	3.7662
Mean	4.1707	2.2382	-5.2892
Standard deviation	0.4467	0.2546	2.9009
(b) Explanatory variables	Ec _{<i>t</i>}	Ob _{<i>t</i>}	Pr _{<i>t</i>}
Variable	Eccentricity of Earth's orbit	Obliquity	Precession of the equinox
Data frequency	1,000 years	1,000 years	1,000 years
Measurement	Periodicity deriving from the changing non-circularity of Earth's orbit (zero denotes circularity).	Periodicity deriving from the changes in the tilt of Earth's rotational axis relative to the ecliptic (1 unit = 10 degrees).	Periodicity deriving from the precession of the equinox (1 unit = 1 degree).
Data source	Paillard et al. (1996)	Paillard et al. (1996)	Paillard et al. (1996)
Descriptive statistics for the explanatory variables for the historical period:			
Start date	798,000 years ago	798,000 years ago	798,000 years ago
End date	1,000 years ago	1,000 years ago	1,000 years ago
Sample size	798	798	798
Minimum	0.0042	2.2076	0.0008
Maximum	0.0500	2.4455	0.3593
Mean	0.0271	2.3342	0.1802
Standard deviation	0.0119	0.0591	0.1039

(GDP) has a normal distribution, which may not be satisfied in practical applications.

In the work of Castle and Hendry (2020), estimation and forecasting results are presented for a general unrestricted model (GUM), named the ice-age model. In the work of Blazsek and Escribano (2022), the score-driven ice-age model is introduced. Those authors show that the statistical performance of their model is superior to the statistical performance of the ice-age model of Castle and Hendry (2020). Nevertheless, Blazsek and Escribano (2022) also show that the forecasting performance of the score-driven ice-age model does not improve the forecasting performance of the ice-age model of Castle and Hendry (2020). Blazsek and Escribano (2022) find that the multi-step ahead forecasting results for the climate variables indicate that both models fail to predict well the evolution of climate variables for the last 10,000 to 15,000 years, when humanity has influenced Earth's climate. On the forecasting results, see Castle and Hendry (2020, p. 111) and Blazsek and Escribano (2022).

The starting point of the econometric modeling of this paper is the score-driven homoskedastic ice-age model of Blazsek and Escribano (2022). Our objective is to improve the statistical and forecasting performances of that model, in order to forecast the climate variables for the forthcoming 5000 years, and predict whether we can expect a turning point in global warming within that period. The dependent variables y_t (3×1) of the ice-age model are $y_t = (Ice_t, CO_{2,t}, Temp_t)'$ for $t = 1, \dots, T$, where Ice_t denotes global ice volume, $CO_{2,t}$ denotes atmospheric carbon dioxide level, and $Temp_t$ denotes Antarctic-based land surface temperature. The order of the variables in y_t is defined in the work of Castle and Hendry (2020). In the remainder of this section, we review the score-driven ice-age model:

$$y_t = \mu_t + v_t \tag{1}$$

$$\mu_t = \gamma_0 + \Gamma_1 \mu_{t-1} + \Gamma_2 z_t + \Gamma_3 z_{t-1} + \Psi u_{t-1} \tag{2}$$

where $v_t \sim t_3(0, \Sigma, \nu)$ is the reduced-form error term which has a multivariate i.i.d. t -distribution, where the scale matrix is $\Sigma \equiv \Omega \Omega'$

(3×3), for which Ω (3×3) is a lower-triangular squared matrix with positive elements in the diagonal, and $\nu > 2$ is the degrees of freedom parameter (the restriction on the parameter space $\nu > 2$ ensures that the covariance matrix of v_t is well-defined). The variance of the reduced-form error term is factorized, as follows:

$$\text{Var}(v_t) = \Sigma \times \frac{\nu}{\nu - 2} = \left(\frac{\nu}{\nu - 2}\right)^{1/2} \times \Omega \Omega' \times \left(\frac{\nu}{\nu - 2}\right)^{1/2} \tag{3}$$

Based on that, the following multivariate i.i.d. structural-form error term ϵ_t is introduced:

$$v_t = \left(\frac{\nu}{\nu - 2}\right)^{1/2} \Omega \times \epsilon_t \tag{4}$$

where $E(\epsilon_t) = 0$, $\text{Var}(\epsilon_t) = I_3$ and $\epsilon_t \sim t_3[0, I_3 \times (\nu - 2)/\nu, \nu]$.

Moreover, μ_t (3×1) is the conditional mean of y_t given $\mathcal{F}_{t-1} \equiv (y_1, \dots, y_{t-1}, z_1, \dots, z_t)$, u_t (3×1) is the vector of scaled score functions (Harvey, 2013), and z_t (9×1) is the vector of strictly exogenous explanatory variables. The assumption of strict exogeneity of z_t for score-driven models is from the work of Harvey (2013, p. 56), which is supported in the work of Castle and Hendry (2020, p. 95). The elements of z_t are three main interacting orbital changes over time affecting solar radiation that could drive ice ages (Castle and Hendry, 2020):

$$z_t = (Ec_t, Ob_t, Pr_t, Ec_t \times Ob_t, Ec_t \times Pr_t, Ob_t \times Pr_t, Ec_t^2, Ob_t^2, Pr_t^2)' \tag{5}$$

where 'Ec' measures the eccentricity (i.e., non-circularity) of Earth's orbit, 'Ob' is obliquity measuring the tilt of Earth's rotational axis relative to the ecliptic, and 'Pr' is a measure of the precession of the equinox (i.e., circular rotation of the rotational axis itself).

The conditional mean μ_t includes the following parameters: the vector of constant parameters γ_0 (3×1), and the parameter matrices Γ_1 (3×3), Γ_2 (3×9), Γ_3 (3×9), and Ψ (3×3). We assume that the maximum modulus of the eigenvalues of Γ_1 is less than one, which ensures that μ_t is asymptotically covariance stationary (Harvey, 2013; Blasques et al., 2022; Blazsek et al., 2022a,b). We initialize μ_t by using the start values of the dependent variables y_1 .

For Γ_1 , Γ_2 , and Γ_3 , we use the same restrictions as in the work of Castle and Hendry (2020), which is also motivated by the general-to-specific model selection procedure for the score-driven ice-age model

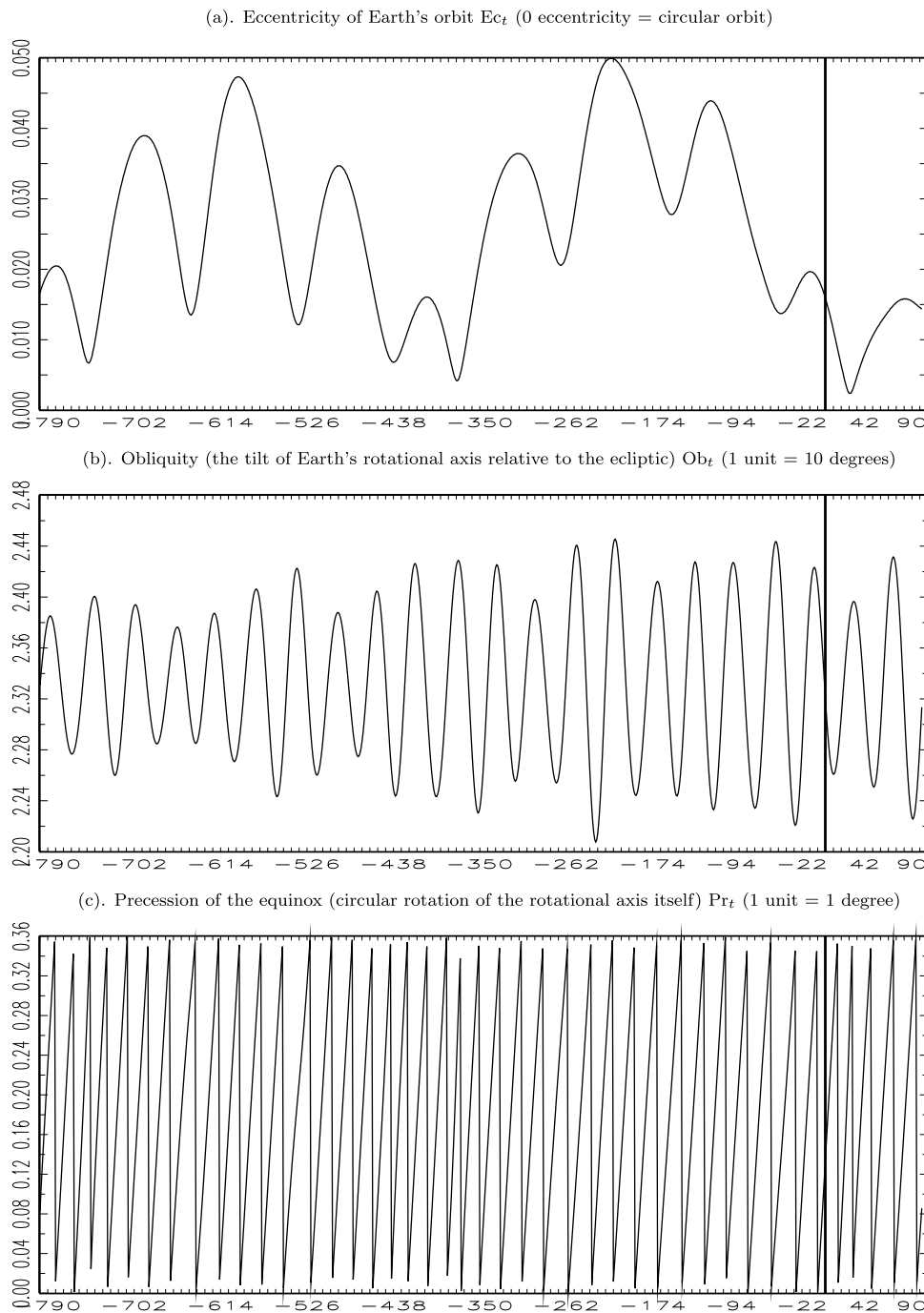


Fig. 2. Evolution of Ec_t , Ob_t , and Pr_t from 798,000 years ago to 100,000 years in the future. *Note:* In each panel a vertical thick line divides the past and the future. From the future data, we focus on the forthcoming 5000 years of data for the out-of-sample predictions in this paper. *Source:* [Castle and Hendry \(2020\)](#).

explained in the work of [Blazsek and Escribano \(2022\)](#). Moreover, the same elements of Γ_1 and Ψ are restricted for the score-driven models as for matrix Γ_1 in the work of [Castle and Hendry \(2020\)](#). According to [Castle and Hendry \(2020, p. 104\)](#), the following elements of Γ_1 are not restricted to zero: $\Gamma_{1,1,1}$, $\Gamma_{1,1,3}$, $\Gamma_{1,2,2}$, $\Gamma_{1,2,3}$, $\Gamma_{1,3,2}$, and $\Gamma_{1,3,3}$. The following elements of Γ_2 are not restricted to zero: $\Gamma_{2,1,1}$, $\Gamma_{2,1,4}$, $\Gamma_{2,1,5}$, $\Gamma_{2,2,1}$, $\Gamma_{2,2,8}$, $\Gamma_{2,3,1}$, $\Gamma_{2,3,4}$, and $\Gamma_{2,3,5}$. Moreover, the following elements of Γ_3 are also not restricted to zero: $\Gamma_{3,1,1}$, $\Gamma_{3,1,2}$, $\Gamma_{3,1,4}$, $\Gamma_{3,2,1}$, $\Gamma_{3,2,2}$, $\Gamma_{3,2,4}$, and $\Gamma_{3,3,4}$.

For the interpretation of the parameter estimates in μ_t , we present the specification of the conditional location under the aforementioned

restrictions:

$$\begin{aligned} \mu_{ice,t} = & \gamma_{0,1} + \Gamma_{1,1,1}\mu_{ice,t-1} + \Gamma_{1,1,3}\mu_{Temp,t-1} \\ & + \Gamma_{2,1,1}Ec_t + \Gamma_{2,1,4}(Ec_t \times Ob_t) + \Gamma_{2,1,5}(Ec_t \times Pr_t) \\ & + \Gamma_{3,1,1}Ec_{t-1} + \Gamma_{3,1,2}Ob_{t-1} + \Gamma_{3,1,4}(Ec_{t-1} \times Ob_{t-1}) \\ & + \Psi_{1,1}u_{1,t-1} + \Psi_{1,3}u_{3,t-1} \end{aligned} \tag{6}$$

$$\begin{aligned} \mu_{CO_2,t} = & \gamma_{0,2} + \Gamma_{1,2,2}\mu_{CO_2,t-1} + \Gamma_{1,2,3}\mu_{Temp,t-1} \\ & + \Gamma_{2,2,1}Ec_t + \Gamma_{2,1,8} \times Ob_t^2 \\ & + \Gamma_{3,2,1}Ec_{t-1} + \Gamma_{3,2,2}Ob_{t-1} + \Gamma_{3,2,4}(Ec_{t-1} \times Ob_{t-1}) \\ & + \Psi_{2,2}u_{2,t-1} + \Psi_{2,3}u_{3,t-1} \end{aligned} \tag{7}$$

$$\begin{aligned} \mu_{\text{Temp},t} &= \gamma_{0,3} + \Gamma_{1,3,2} \mu_{\text{CO}_2,t-1} + \Gamma_{1,3,3} \mu_{\text{Temp},t-1} \\ &+ \Gamma_{2,3,1} \text{Ec}_t + \Gamma_{2,3,4} (\text{Ec}_t \times \text{Ob}_t) + \Gamma_{2,3,5} (\text{Ec}_t \times \text{Pr}_t) \\ &+ \Gamma_{3,3,4} (\text{Ec}_{t-1} \times \text{Ob}_{t-1}) \\ &+ \Psi_{3,2} \mu_{2,t-1} + \Psi_{3,3} \mu_{3,t-1} \end{aligned} \quad (8)$$

Eqs. (6) to (8) can also be used for the interpretation of parameters for the score-driven MS ice-age model (Section 3.2) and the score-driven threshold ice-age model (Section 3.3).

The scaled score function u_t is defined as follows. The log of the conditional density of y_t is:

$$\begin{aligned} \ln f(y_t | \mathcal{F}_{t-1}; \Theta) &= \ln \Gamma \left(\frac{\nu+3}{2} \right) - \ln \Gamma \left(\frac{\nu}{2} \right) - \frac{3}{2} \ln(\pi\nu) - \frac{1}{2} \ln |\Sigma| \\ &- \frac{\nu+3}{2} \ln \left[1 + \frac{v_t' \Sigma^{-1} v_t}{\nu} \right] \end{aligned} \quad (9)$$

where $v_t = y_t - \mu_t$, $\Theta = (\Theta_1, \dots, \Theta_S)'$ is the vector of time-invariant parameters, which includes the elements of γ_0 , Γ_1 , Γ_2 , Γ_3 , Ψ , Ω , and ν . The partial derivative of the log conditional density $\ln f(y_t | \mathcal{F}_{t-1}; \Theta)$ with respect to μ_t is (Harvey, 2013):

$$\frac{\partial \ln f(y_t | \mathcal{F}_{t-1}; \Theta)}{\partial \mu_t} = \frac{\nu+3}{\nu} \Sigma^{-1} \times \left(1 + \frac{v_t' \Sigma^{-1} v_t}{\nu} \right)^{-1} v_t \equiv \frac{\nu+3}{\nu} \Sigma^{-1} \times u_t \quad (10)$$

The scaled score function u_t is defined in the second equality of Eq. (10), where v_t is multiplied by $[1 + (v_t' \Sigma^{-1} v_t)/\nu]^{-1} = \nu/(\nu + v_t' \Sigma^{-1} v_t) \in (0, 1)$. Therefore, the scaled score function is bounded by the reduced-form error term: $|u_t| < |v_t|$. All elements of u_t are bounded functions of v_t for $\nu < \infty$ (Harvey, 2013), hence all moments of u_t are well-defined. In the work of Harvey (2013), it is shown that u_t is multivariate i.i.d. with mean zero and a covariance matrix:

$$\text{Var}(u_t) = E \left[\frac{\partial \ln f(y_t | \mathcal{F}_{t-1}; \Theta)}{\partial \mu_t} \times \frac{\partial \ln f(y_t | \mathcal{F}_{t-1}; \Theta)}{\partial \mu_t'} \right] = \frac{\nu+3}{\nu+5} \times \Sigma^{-1} \quad (11)$$

In Fig. 3, we present the scaled score function u_t as a function of $\epsilon_{1,t}$. The figure presents u_t for the estimates for the score-driven ice-age model. In the three-dimensional graphs of Fig. 3, we present the elements of u_t as functions of $\epsilon_{1,t}$ and $\epsilon_{2,t}$, where $\epsilon_{3,t} = 0$ for the purpose of illustration. The figure indicates that the score-driven ice-age model is robust to extreme observations.

One of the reasons why the score-driven ice-age model (Blazsek and Escribano, 2022) and the ice-age model (Castle and Hendry, 2020) are not able to predict well the climate variables for the last 10,000 to 15,000 years, when humanity has influenced Earth's climate, is that they do not account for possible structural changes in the climate DGP. In the following section, we present a MS model for the climate data to motivate the use of structural changes in climate-econometric models.

3.2. Score-driven Markov-switching (MS) ice-age model

In this section, we introduce the score-driven MS ice-age model, and we provide evidence of structural changes in the climate, indicating periods of sharply increasing $\text{CO}_{2,t}$ and Temp_t . We extend the single-regime score-driven ice-age model as follows:

$$y_t = \mu_t(s_t) + v_t(s_t) \quad (12)$$

$$\mu_t(s_t) = \gamma_0(s_t) + \Gamma_1(s_t) \mu_{t-1}(s_t) + \Gamma_2(s_t) z_t + \Gamma_3(s_t) z_{t-1} + \Psi(s_t) u_{t-1}(s_t) \quad (13)$$

for regimes $s_t = 1, 2$ and $t = 1, \dots, T$. The regime variable s_t is a Markov process with the following time-invariant transition probability parameters: $\Pr(s_t = 1 | s_{t-1} = 1) = p$ and $\Pr(s_t = 2 | s_{t-1} = 2) = q$. The time-invariant probabilities of regimes are given by: $\pi_1^* = \Pr(s_t = 1) = (1-q)/(2-p-q)$ and $\pi_2^* = \Pr(s_t = 2) = (1-p)/(2-p-q)$. The asymptotic covariance stationarity of y_t is provided if the maximum modulus of

all the eigenvalues of $\Gamma_1(s_t)$ for $s_t = 1, 2$ is less than one, where we denote the maximum moduli for the two regimes by using C_1 and C_2 , respectively. This is a relatively strict condition because it requires that both regimes are asymptotically covariance stationary. Therefore, we also use a less restrictive condition of asymptotic covariance stationarity from the work of Blazsek et al. (2021), which allows that one of the regimes is non-stationary. We define the matrix:

$$A = \begin{bmatrix} \Gamma_1(1) \frac{\pi_1^*}{\pi_1^*} p & \Gamma_1(1) \frac{\pi_2^*}{\pi_1^*} (1-q) \\ \Gamma_1(2) \frac{\pi_1^*}{\pi_2^*} (1-p) & \Gamma_1(2) \frac{\pi_2^*}{\pi_2^*} q \end{bmatrix} = \begin{bmatrix} \Gamma_1(1) p & \Gamma_1(1) \frac{\pi_2^*}{\pi_1^*} (1-q) \\ \Gamma_1(2) \frac{\pi_1^*}{\pi_2^*} (1-p) & \Gamma_1(2) q \end{bmatrix} \quad (14)$$

The dependent variable y_t in the score-driven MS ice-age model is asymptotically covariance stationary if the maximum modulus of all the eigenvalues of A , denoted as C_{Stat} , is less than one.

The error term $v_t(s_t) \sim t_3[0, \Sigma(s_t), \nu(s_t)]$ has a multivariate i.i.d. t -distribution, where the scale matrix is $\Sigma(s_t) \equiv \Omega(s_t) \Omega(s_t)'$ (3×3), for which $\Omega(s_t)$ (3×3) is a lower-triangular squared matrix with positive elements in the diagonal, and $\nu(s_t) > 2$ is the degrees of freedom parameter.

The filter $\mu_t(s_t)$ (3×1) is the conditional mean of $y_t | (\mathcal{F}_{t-1}, s_t) \equiv y_t | (y_1, \dots, y_{t-1}, z_1, \dots, z_t, s_t)$. We initialize the conditional mean $\mu_t(s_t)$ for both regimes by using the start values of the dependent variables y_1 . The regime-switching conditional mean $\mu_t(s_t)$ includes the following parameters: the vector of parameters $\gamma_0(s_t)$ (3×1), and the parameter matrices $\Gamma_1(s_t)$ (3×3), $\Gamma_2(s_t)$ (3×9), $\Gamma_3(s_t)$ (3×9), and $\Psi(s_t)$ (3×3). For $\Gamma_1(s_t)$, $\Gamma_2(s_t)$, $\Gamma_3(s_t)$, and $\Psi(s_t)$ we use the same restrictions as for the single-regime score-driven homoskedastic ice-age model (Blazsek and Escribano, 2022).

In Eq. (13), the filter is updated by z_t (9×1), the first lag of z_t , and the conditional mean of the first lags of $\mu_t(s_t)$ and $u_t(s_t)$ (both 3×1), where the latter is the regime-switching vector of scaled score functions. The updating terms of $\mu_t(s_t)$ are defined as $\mu_{t-1}(s_t) = E[\mu_{t-1}(s_{t-1}) | \mathcal{F}_{t-1}, s_t]$ and $u_{t-1}(s_t) = E[u_{t-1}(s_{t-1}) | \mathcal{F}_{t-1}, s_t]$. The computation of these conditional expectations for score-driven models is presented in the work of Blazsek et al. (2021).

The scaled score function $u_t(s_t)$ is defined as follows. The log conditional density of y_t is:

$$\ln f(y_t | \mathcal{F}_{t-1}, s_t; \Theta) = \ln \Gamma \left[\frac{\nu(s_t)+3}{2} \right] - \ln \Gamma \left[\frac{\nu(s_t)}{2} \right] - \frac{3}{2} \ln[\pi\nu(s_t)] \quad (15)$$

$$- \frac{1}{2} \ln |\Sigma(s_t)| - \frac{\nu(s_t)+3}{2} \ln \left\{ 1 + \frac{v_t(s_t)' [\Sigma(s_t)]^{-1} v_t(s_t)}{\nu(s_t)} \right\}$$

where $v_t(s_t) = y_t - \mu_t(s_t)$, $\Theta = (\Theta_1, \dots, \Theta_S)'$ is the vector of time-invariant parameters, which includes the elements of $\gamma_0(s_t)$, $\Gamma_1(s_t)$, $\Gamma_2(s_t)$, $\Gamma_3(s_t)$, $\Psi(s_t)$, $\Omega(s_t)$, and $\nu(s_t)$. The partial derivative of the log conditional density $\ln f(y_t | \mathcal{F}_{t-1}, s_t; \Theta)$ with respect to $\mu_t(s_t)$ is:

$$\begin{aligned} &\frac{\partial \ln f(y_t | \mathcal{F}_{t-1}, s_t; \Theta)}{\partial \mu_t(s_t)} \\ &= \frac{\nu(s_t)+3}{\nu(s_t)} [\Sigma(s_t)]^{-1} \times \left\{ 1 + \frac{v_t(s_t)' [\Sigma(s_t)]^{-1} v_t(s_t)}{\nu(s_t)} \right\}^{-1} v_t(s_t) \quad (16) \\ &\equiv \frac{\nu(s_t)+3}{\nu(s_t)} [\Sigma(s_t)]^{-1} \times u_t(s_t) \end{aligned}$$

The score-driven MS ice-age model is estimated by using the ML method (Blazsek et al., 2021). We note that the conditional distribution of y_t depends only on the contemporaneous regime s_t , which greatly simplifies the statistical inference of the model.

For the empirical results reported in this paper only parameters $\gamma_0(s_t)$ and $\Gamma_1(s_t)$ are regime-switching. This is a result of an extensive work on a general-to-specific approach involving a large number of estimations of alternative score-driven MS ice-age model specifications, to determine which parameters should be regime-switching to effectively separate the regimes. We start with the most general version of the MS

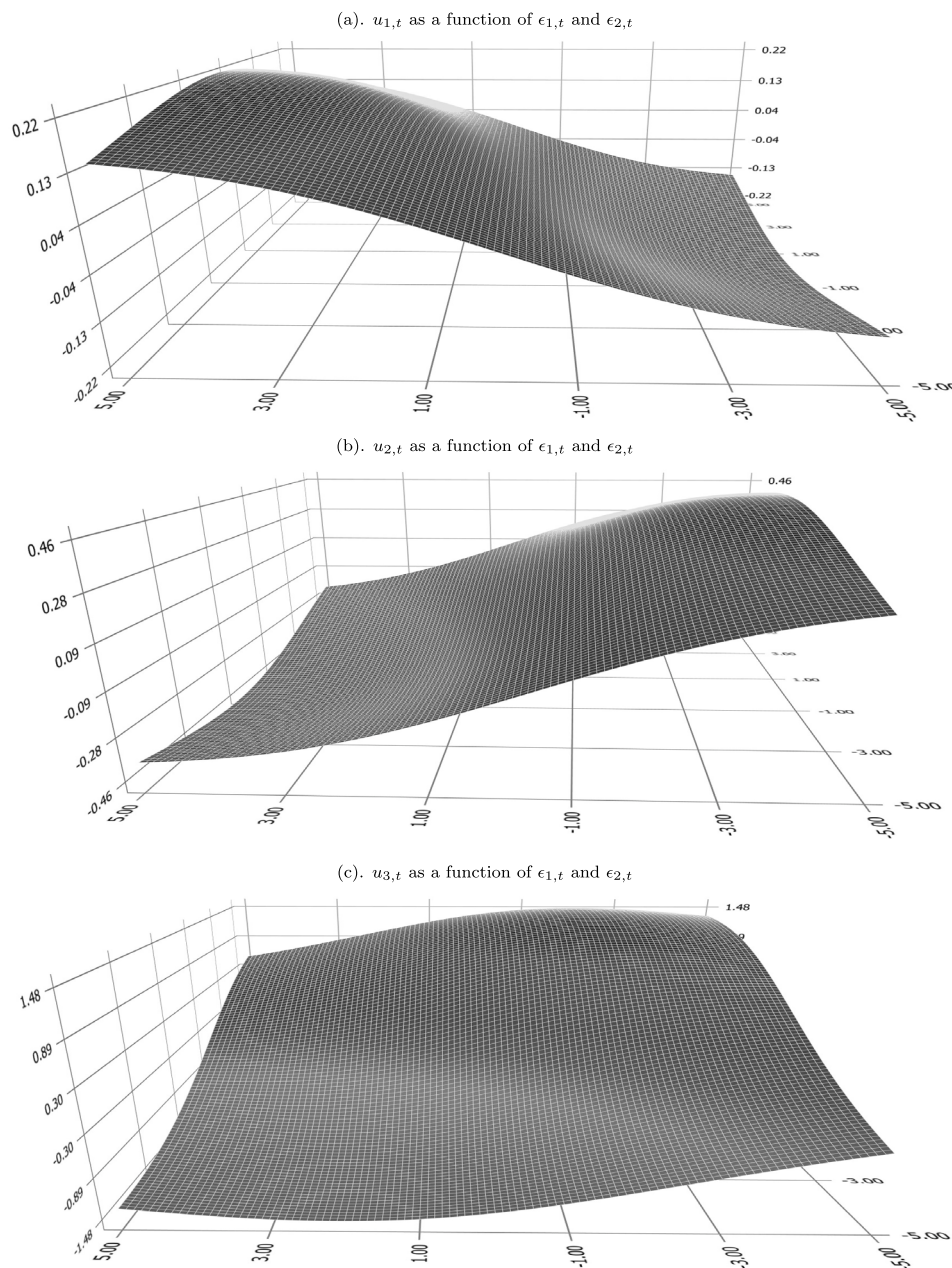


Fig. 3. Robustness of the scaled score function to extreme values. Note: $\epsilon_{3,t} = 0$ is assumed for this figure.

model in which all parameters of the score-driven ice-age model are regime-switching. We impose single-regime restrictions on the parameters step-by-step, until we find the best-performing MS specification, in which only $\gamma_0(s_t)$ and $\Gamma_1(s_t)$ are regime-switching. Moreover, we assume that there are two latent states $s_t \in \{1, 2\}$, which is supported by using a likelihood ratio (LR) test for MS models (Kawahara and Shimotsu, 2018) in a preliminary analysis.

In Table 2(a), by using the estimation window for the period of 798,000 years ago to 1000 years ago, we present the parameter estimates and diagnostic test results for the score-driven MS ice-age model. The C_1 , C_2 , and C_{Stat} statistics indicate that y_t is covariance stationary. The Ljung–Box (LB) tests (Ljung and Box, 1978) for v_t and u_t indicate that all elements of those vectors form an independent time series. These diagnostic test results support the MS specification.

We use the score-driven MS ice-age model to show evidence of structural changes in the climate variables, which are not captured by the ice-age model (Castle and Hendry, 2020) and the score-driven

ice-age model (Blazsek and Escribano, 2022). In Fig. 4, by using the estimation window for the period of 798,000 years ago to 1000 years ago, we present the evolution of the smoothed probability of $s_t = 1$, i.e., $\bar{\pi}_{1,t} = \Pr(s_t = 1 | y_1, \dots, y_T)$, and climate variables Ice_t , $\text{CO}_{2,t}$, and Temp_t for the period of 798,000 years ago to 1000 years ago. We note that the computation of $\bar{\pi}_{1,t}$ for score-driven MS models is presented in the work of Blazsek et al. (2021). Fig. 4 indicates that $s_t = 1$ is associated with sharp increases in the Atmospheric carbon dioxide level $\text{CO}_{2,t}$ and Antarctic-based land surface temperature Temp_t , for which we find that $s_t = 1$ is not persistent. On the other hand, $s_t = 2$ indicates the rest of the time periods, for which we find that $s_t = 2$ is highly persistent and dominates most of the observation period. The results indicate structural changes for the variables Ice_t , $\text{CO}_{2,t}$, and Temp_t .

3.3. Score-driven threshold ice-age model

Motivated by the results on the score-driven MS ice-age model, we cluster the climate observations using Ward's linkage clustering

Table 2

In-sample estimates for the score-driven Markov-switching (MS) ice-age model, and the score-driven threshold ice-age model for two clusters with respect to Temp_{*t*}, where the latter specification provides the most accurate forecasts for the last 20,000 years) (see Table 3), for the period of 798,000 years ago to 1000 years ago.

(a). Score-driven Markov-switching ice-age model			(b). Score-driven threshold ice-age model with clustering with respect to Temp _{<i>t</i>}						
Regime 1 = sharply increasing Temp _{<i>t</i>} ; Regime 2 = otherwise			Regime 1 = low Temp _{<i>t</i>} ; regime 2 = high Temp _{<i>t</i>}						
$\gamma_{0,1}(1)$	1.7945*** (0.3198)	$\gamma_{0,1}(2)$	1.1154*** (0.2584)	$\gamma_{0,1}(1)$	2.8696*** (0.9571)	$\gamma_{0,1}(2)$	0.8702*** (0.2883)	C_1	0.8376
$\gamma_{0,2}(1)$	1.2341*** (0.3597)	$\gamma_{0,2}(2)$	1.1293*** (0.3149)	$\gamma_{0,2}(1)$	3.8581*** (1.0618)	$\gamma_{0,2}(2)$	1.3515*** (0.4151)	C_2	0.9074
$\gamma_{0,3}(1)$	-8.4994*** (2.6519)	$\gamma_{0,3}(2)$	-1.0862 (0.8078)	$\gamma_{0,3}(1)$	5.4906* (3.0986)	$\gamma_{0,3}(2)$	-1.9692** (0.9585)	LB $v_{1,t}$	20.3465 (0.8515)
$\Gamma_{1,1,1}(1)$	0.7010*** (0.0520)	$\Gamma_{1,1,1}(2)$	0.9127*** (0.0155)	$\Gamma_{1,1,1}(1)$	0.8376*** (0.0351)	$\Gamma_{1,1,1}(2)$	0.8947*** (0.0185)	LB $v_{2,t}$	27.5458 (0.4887)
$\Gamma_{1,1,3}(1)$	-0.0416*** (0.0078)	$\Gamma_{1,1,3}(2)$	-0.0117*** (0.0024)	$\Gamma_{1,1,3}(1)$	-0.0138** (0.0068)	$\Gamma_{1,1,3}(2)$	-0.0134*** (0.0037)	LB $v_{3,t}$	30.5789 (0.3361)
$\Gamma_{1,2,2}(1)$	0.8689*** (0.0694)	$\Gamma_{1,2,2}(2)$	0.8656*** (0.0222)	$\Gamma_{1,2,2}(1)$	0.5346*** (0.0871)	$\Gamma_{1,2,2}(2)$	0.8582*** (0.0298)	LB $u_{1,t}$	22.0181 (0.7805)
$\Gamma_{1,2,3}(1)$	0.0080 (0.0056)	$\Gamma_{1,2,3}(2)$	0.0096*** (0.0021)	$\Gamma_{1,2,3}(1)$	0.0329*** (0.0082)	$\Gamma_{1,2,3}(2)$	0.0096*** (0.0035)	LB $u_{2,t}$	25.6766 (0.5908)
$\Gamma_{1,3,2}(1)$	3.3994*** (1.0233)	$\Gamma_{1,3,2}(2)$	0.2473 (0.2959)	$\Gamma_{1,3,2}(1)$	-1.9465* (1.1069)	$\Gamma_{1,3,2}(2)$	0.3553 (0.3342)	LB $u_{3,t}$	34.7165 (0.1783)
$\Gamma_{1,3,3}(1)$	0.6442*** (0.0818)	$\Gamma_{1,3,3}(2)$	0.9112*** (0.0278)	$\Gamma_{1,3,3}(1)$	0.9392*** (0.1024)	$\Gamma_{1,3,3}(2)$	0.8380*** (0.0422)	LL	1.6927
$\Gamma_{2,1,1}$	87.5148*** (26.5560)	ρ	0.4412*** (0.0749)	$\Gamma_{2,1,1}(1)$	-31.4162 (107.6720)	$\Gamma_{2,1,1}(2)$	87.3692*** (33.3199)	AIC	-3.1999
$\Gamma_{2,1,4}$	-45.3373** (10.9720)	q	0.9384*** (0.0120)	$\Gamma_{2,1,4}(1)$	1.0635 (45.2982)	$\Gamma_{2,1,4}(2)$	-44.1306*** (13.7167)	BIC	-2.7657
$\Gamma_{2,1,5}$	-5.1217*** (0.9538)	C_1	0.9563	$\Gamma_{2,1,5}(1)$	-4.7914** (2.1320)	$\Gamma_{2,1,5}(2)$	-5.3557** (1.1671)	HQC	-3.0330
$\Gamma_{2,2,1}$	12.6727*** (3.6288)	C_2	0.9421	$\Gamma_{2,2,1}(1)$	-0.7702 (18.3994)	$\Gamma_{2,2,1}(2)$	14.6027** (4.8421)		
$\Gamma_{2,2,8}$	0.0765* (0.0459)	C_{Stat}	0.9478	$\Gamma_{2,2,8}(1)$	0.4307*** (0.1532)	$\Gamma_{2,2,8}(2)$	0.1035* (0.0590)		
$\Gamma_{2,3,1}$	-335.7532*** (37.3845)	LB $v_{1,t}$	20.4634 (0.8470)	$\Gamma_{2,3,1}(1)$	-321.9976** (103.6567)	$\Gamma_{2,3,1}(2)$	-241.2780*** (46.3039)		
$\Gamma_{2,3,4}$	243.1959*** (27.2797)	LB $v_{2,t}$	27.4371 (0.4946)	$\Gamma_{2,3,4}(1)$	242.9438** (102.8331)	$\Gamma_{2,3,4}(2)$	192.9595*** (31.0481)		
$\Gamma_{2,3,5}$	28.5945*** (7.5770)	LB $v_{3,t}$	37.0713 (0.1173)	$\Gamma_{2,3,5}(1)$	13.8527 (12.9534)	$\Gamma_{2,3,5}(2)$	32.0467*** (8.9383)		
$\Gamma_{3,1,1}$	-83.5604*** (28.1047)	LB $u_{1,t}$	20.3781 (0.8503)	$\Gamma_{3,1,1}(1)$	15.5797 (120.0182)	$\Gamma_{3,1,1}(2)$	-73.2639** (34.7783)		
$\Gamma_{3,1,2}$	-0.3420*** (0.1046)	LB $u_{2,t}$	25.4290 (0.6044)	$\Gamma_{3,1,2}(1)$	-0.9883** (0.3897)	$\Gamma_{3,1,2}(2)$	-0.2061* (0.1153)		
$\Gamma_{3,1,4}$	43.8732*** (11.6186)	LB $u_{3,t}$	37.1578 (0.1154)	$\Gamma_{3,1,4}(1)$	6.3876 (49.7383)	$\Gamma_{3,1,4}(2)$	38.2138*** (14.3819)		
$\Gamma_{3,2,1}$	-30.8272*** (6.2538)	LL	1.6837	$\Gamma_{3,2,1}(1)$	-0.8960 (25.5736)	$\Gamma_{3,2,1}(2)$	-32.7165*** (8.5696)		
$\Gamma_{3,2,2}$	-0.5120** (0.2238)	AIC	-3.2472	$\Gamma_{3,2,2}(1)$	-2.1019** (0.7590)	$\Gamma_{3,2,2}(2)$	-0.6669** (0.2911)		
$\Gamma_{3,2,4}$	7.6086*** (2.0094)	BIC	-2.9656	$\Gamma_{3,2,4}(1)$	-0.0189 (6.8009)	$\Gamma_{3,2,4}(2)$	7.9011** (3.0940)		
$\Gamma_{3,3,4}$	-101.9864*** (22.3188)	HQC	-3.1390	$\Gamma_{3,3,4}(1)$	-115.3612 (97.7131)	$\Gamma_{3,3,4}(2)$	-88.9701*** (25.2036)		
$\Psi_{1,1,1}$	0.8551*** (0.0445)			$\Psi_{1,1,1}(1)$	0.9704*** (0.1246)	$\Psi_{1,1,1}(2)$	0.8866*** (0.0497)		
$\Psi_{1,1,3}$	-0.0223*** (0.0054)			$\Psi_{1,1,3}(1)$	-0.0360** (0.0143)	$\Psi_{1,1,3}(2)$	-0.0244*** (0.0059)		
$\Psi_{1,2,2}$	1.3508*** (0.0562)			$\Psi_{1,2,2}(1)$	1.0676*** (0.1325)	$\Psi_{1,2,2}(2)$	1.4589*** (0.0688)		
$\Psi_{1,2,3}$	0.0176*** (0.0024)			$\Psi_{1,2,3}(1)$	0.0432*** (0.0104)	$\Psi_{1,2,3}(2)$	0.0141*** (0.0034)		
$\Psi_{1,3,2}$	4.8316*** (0.8794)			$\Psi_{1,3,2}(1)$	1.2620 (1.7254)	$\Psi_{1,3,2}(2)$	5.7135*** (0.8303)		
$\Psi_{1,3,3}$	0.9438*** (0.0455)			$\Psi_{1,3,3}(1)$	1.3422*** (0.1534)	$\Psi_{1,3,3}(2)$	0.8016*** (0.0534)		
$\Omega_{1,1}$	0.0837*** (0.0021)			$\Omega_{1,1}(1)$	0.0874*** (0.0050)	$\Omega_{1,1}(2)$	0.0833*** (0.0024)		
$\Omega_{2,1}$	-0.0041*** (0.0015)			$\Omega_{2,1}(1)$	-0.0124** (0.0052)	$\Omega_{2,1}(2)$	-0.0068*** (0.0021)		
$\Omega_{2,2}$	0.0368*** (0.0010)			$\Omega_{2,2}(1)$	0.0511*** (0.0033)	$\Omega_{2,2}(2)$	0.0439*** (0.0011)		
$\Omega_{3,1}$	-0.1279** (0.0265)			$\Omega_{3,1}(1)$	-0.1171* (0.0604)	$\Omega_{3,1}(2)$	-0.1467*** (0.0336)		
$\Omega_{3,2}$	0.2427** (0.0269)			$\Omega_{3,2}(1)$	0.4059*** (0.0517)	$\Omega_{3,2}(2)$	0.2941*** (0.0291)		
$\Omega_{3,3}$	0.6413*** (0.0153)			$\Omega_{3,3}(1)$	0.5316*** (0.0335)	$\Omega_{3,3}(2)$	0.6479*** (0.0184)		
ν	43.0056*** (7.7986)			$\nu(1)$	20.0801*** (5.6218)	$\nu(2)$	37.6512*** (7.7197)		

Note: $C_1 < 1$ is covariance stationarity of regime 1; $C_2 < 1$ is covariance stationarity of regime 2; $C_{Stat} < 1$ is covariance stationarity of the MS model. The Ljung–Box (LB) statistics (p -values in parentheses) use the lag-order $\sqrt{T} \approx 28$. Log-likelihood (LL); Akaike information criterion (AIC); Bayesian information criterion (BIC); Hannan–Quinn criterion (HQC). Gradient-based standard errors are reported in parentheses.

*Parameter significance at the 10% level.

**Parameter significance at the 5% level.

***Parameter significance at the 1% level.

method. We use Ward’s method because many of the standard clustering methods are special cases of this very general clustering method (Ward, 1963). Ward’s clustering method identifies the different historical periods of abrupt climate changes (periods of structural changes in climate variables), by forming hierarchical combinations of pairs of clusters that minimize the increase in information-loss (error sum of squares for error, SSE) at each step (Everitt, 1993). The use of Ward’s clustering method to specify the score-driven threshold ice-age model is also motivated by its impressive forecasting performance, compared to the forecasting performance of the score-driven MS ice-age model. For a successful application of Ward’s linkage clustering method, we also refer to the works of Blazsek and Escribano (2016a,b). We use Ward’s method for all alternative subsets of the variables Ice_{*t*}, CO_{2,*t*}, and Temp_{*t*} as follows: (i) We cluster with respect to each climate variable (i.e., Ice_{*t*} or CO_{2,*t*} or Temp_{*t*}). (ii) We cluster with respect to all possible pairs of the climate variables (i.e., Ice_{*t*} and CO_{2,*t*}, or Ice_{*t*} and Temp_{*t*}, or CO_{2,*t*} and Temp_{*t*}). (iii) We cluster with respect to the three climate variables (i.e., Ice_{*t*}, CO_{2,*t*}, and Temp_{*t*}). These subsets provide seven ways for the selection of clustering variables, and for each of those we use two and three clusters for the climate variables.

First, two clusters define the dummy variables $D_{1,t}$ and $D_{2,t}$, which indicate a cluster for each observation. We assume that $D_{1,t}$ and $D_{2,t}$ are strictly exogenous. We use the exogeneity assumption for all dummy variables of this paper, because for our dataset we assume that the

structural changes in Earth’s climate are caused by the exogenous orbital variables. We use a general notation for $D_{1,t}$ and $D_{2,t}$, which may represent clustering with respect to any of the aforementioned subsets of Ice_{*t*}, CO_{2,*t*}, and Temp_{*t*}, and formulate the following score-driven threshold ice-age model:

$$y_t = \mu_t + v_t \tag{17}$$

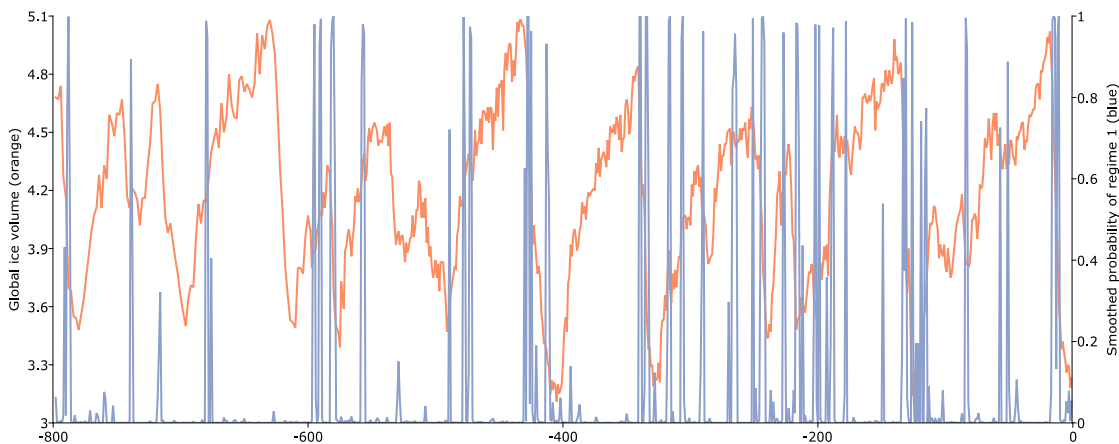
$$\begin{aligned} \mu_t = & \gamma_0(1)D_{1,t} + \gamma_0(2)D_{2,t} + [\Gamma_1(1)D_{1,t} + \Gamma_1(2)D_{2,t}]\mu_{t-1} \\ & + [\Gamma_2(1)D_{1,t} + \Gamma_2(2)D_{2,t}]z_t + [\Gamma_3(1)D_{1,t} + \Gamma_3(2)D_{2,t}]z_{t-1} \\ & + [\Psi(1)D_{1,t} + \Psi(2)D_{2,t}]\mu_{t-1} \end{aligned} \tag{18}$$

$$v_t \sim t_3[0, \Omega(1)\Omega(1)'D_{1,t} + \Omega(2)\Omega(2)'D_{2,t}, \nu(1)D_{1,t} + \nu(2)D_{2,t}] \tag{19}$$

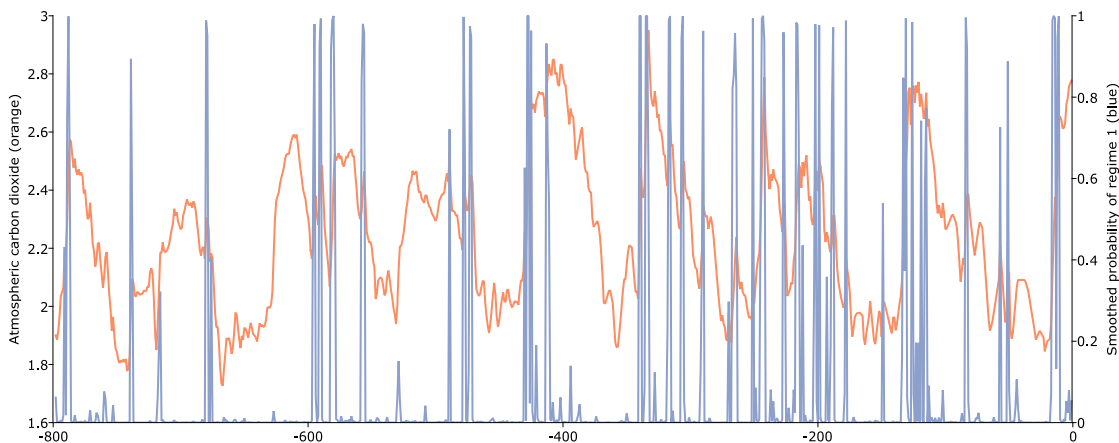
for $t = 1, \dots, T$. The definitions of the variables and parameters and the methods of statistical inference coincide with those for the score-driven ice-age model of Section 3.1.

In Table 2(b), by using the estimation window for the period of 798,000 years ago to 1000 years ago, we present the parameter estimates and diagnostic tests for the score-driven threshold ice-age model, for which two clusters are defined by using the variable Temp_{*t*}. We present the in-sample estimates for this clustering specification in Table 2(b), because its forecasting performance is superior to the forecasting performances of all alternative clustering specifications of

(a). Global ice volume Ice_t and smoothed probability of $s_t = 1$. Correlation: -0.1052



(b). Atmospheric carbon dioxide level $CO_{2,t}$ and smoothed probability of $s_t = 1$. Correlation: 0.2204



(c). Antarctic-based land surface temperature $Temp_t$ and smoothed probability of $s_t = 1$. Correlation: 0.2159

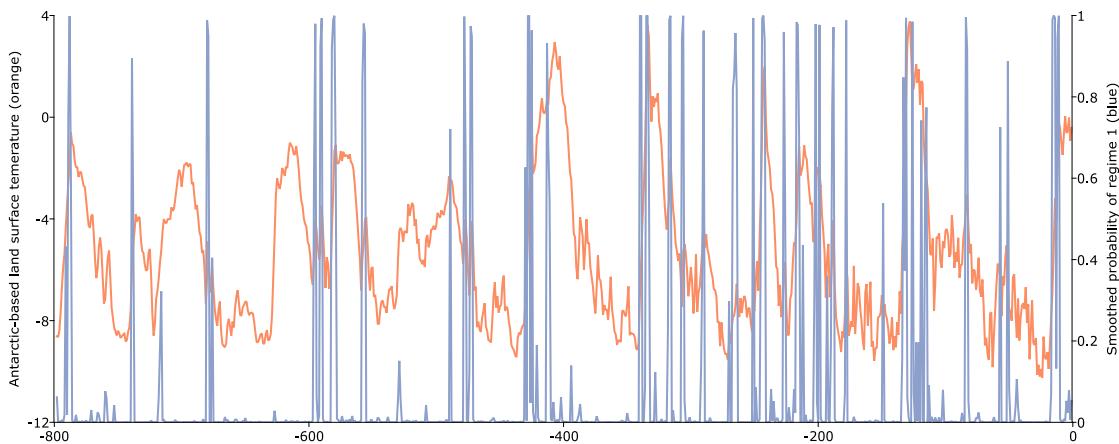


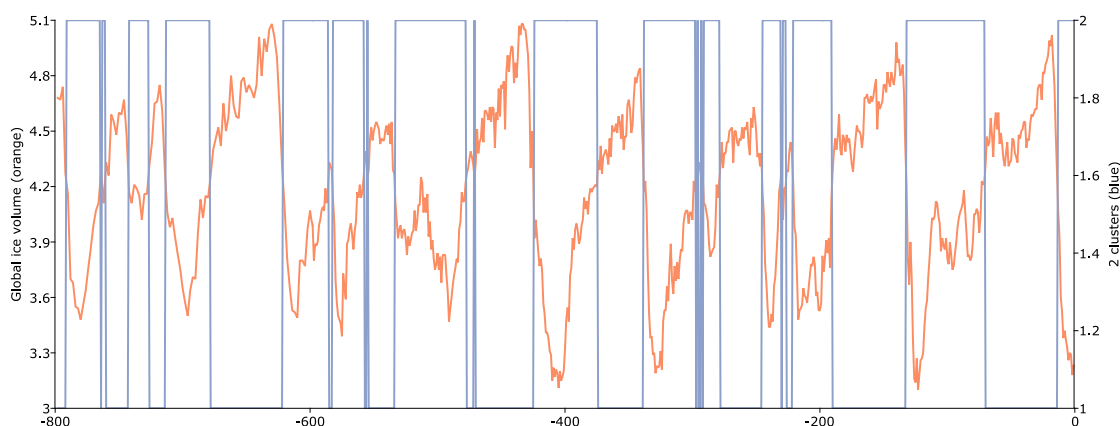
Fig. 4. Ice_t , $CO_{2,t}$, $Temp_t$, and smoothed probability of $s_t = 1$, i.e., $\bar{\pi}_{1,t} = \Pr(s_t = 1 | y_1, \dots, y_T)$, for the score-driven MS ice-age model, from 798,000 years ago to 1000 years ago. Note: Regime s_t is during periods of sharply increasing $CO_{2,t}$ and $Temp_t$.

the score-driven threshold ice-age model for the last 20,000 years (see more on this later in this section for the forecasting results). The C_1 and C_2 statistics indicate that y_t is covariance stationary for both clusters. The LB tests for v_t and u_t indicate that all elements of those vectors form an independent time series. These diagnostic tests support the score-driven threshold ice-age model specification of Table 2(b). We

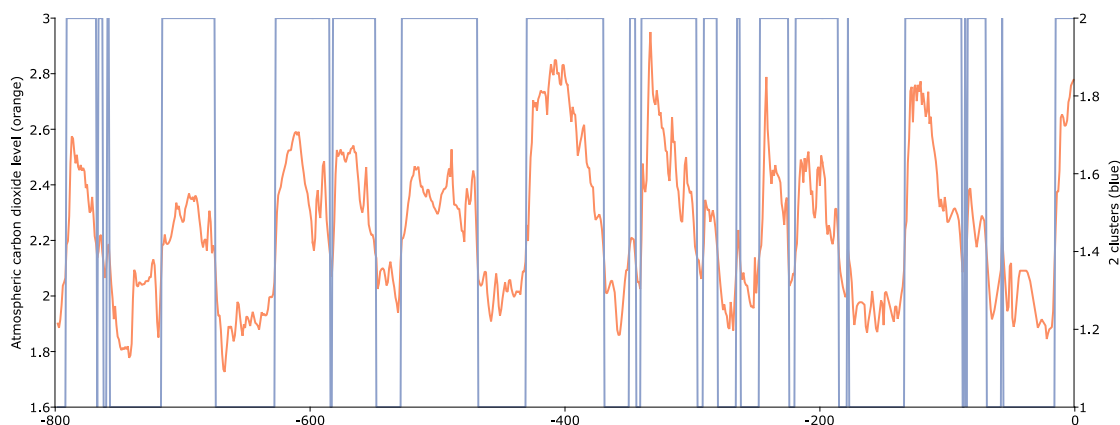
note that, for some alternative specifications of two clusters, the LB test does not support the independence of v_t and u_t .

In Fig. 5, by using the estimation window for the period of 798,000 years ago to 1000 years ago, we present three alternative methods for the definition of two clusters: (i) Ice_t is clustered with respect to Ice_t (Fig. 5(a)), for which $(D_{1,t}, D_{2,t}) = (1, 0)$ indicates a regime with high

(a). Evolution of Ice_t ; two clusters with respect to Ice_t . Cut-point: $Ice_t = 4.2500$.
 Regime 1 is high level of Ice_t ; regime 2 is low level of Ice_t .



(b). Evolution of $CO_{2,t}$; two clusters with respect to $CO_{2,t}$. Cut-point: $CO_{2,t} = 2.1471$.
 Regime 1 is low level of $CO_{2,t}$; regime 2 is high level of $CO_{2,t}$.



(c). Evolution of $Temp_t$; two clusters with respect to $Temp_t$. Cut-point: $Temp_t = -3.1381$.
 Regime 1 is low level of $Temp_t$; regime 2 is high level of $Temp_t$.

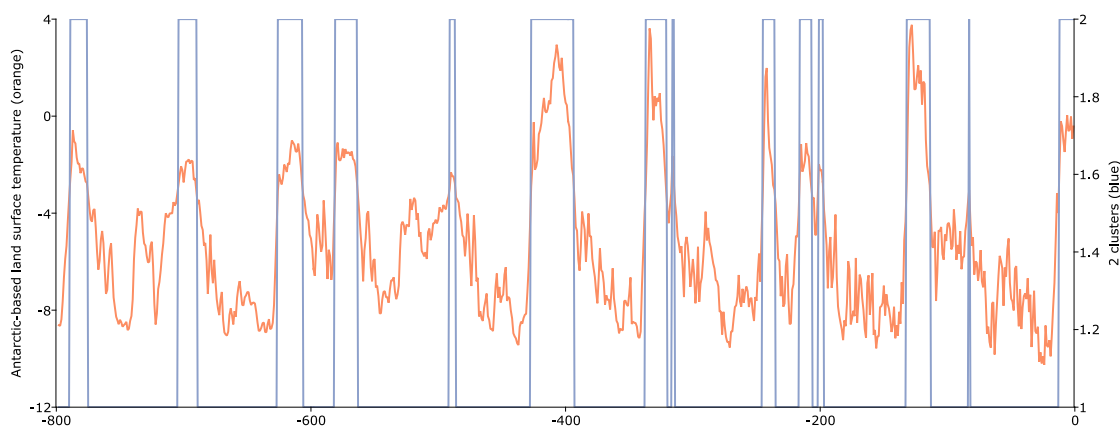


Fig. 5. Ward's linkage clustering for two clusters with respect to each of the three climate variables (i.e., Ice_t , $CO_{2,t}$, and $Temp_t$). *Note:* The best-performing model for two clusters for the forecasting of last the 20,000 years uses $Temp_t$ for clustering for all climate variables (Table 3), which is presented in Panel (c) of this figure.

level of Ice_t , and $(D_{1,t}, D_{2,t}) = (0, 1)$ indicates a regime with low level of Ice_t . (ii) $CO_{2,t}$ is clustered with respect to $CO_{2,t}$ (Fig. 5(b)), for which $(D_{1,t}, D_{2,t}) = (1, 0)$ indicates low level of $CO_{2,t}$, and $(D_{1,t}, D_{2,t}) = (0, 1)$ indicates high level of $CO_{2,t}$. (iii) $Temp_t$ is clustered with respect to $Temp_t$ (Fig. 5(c)), for which $(D_{1,t}, D_{2,t}) = (1, 0)$ indicates a regime with low level of $Temp_t$, and $(D_{1,t}, D_{2,t}) = (0, 1)$ indicates high level

of $Temp_t$. The forecasting performance of clustering with respect to $Temp_t$ (Fig. 5(c)) is superior to the forecasting performances of the alternatives, for the last 20,000 years of our sample.

Second, three clusters define the dummy variables $D_{1,t}$, $D_{2,t}$, and $D_{3,t}$, which indicate a cluster for each observation. We assume that $D_{1,t}$, $D_{2,t}$, and $D_{3,t}$ are strictly exogenous. We use a general notation for the

Table 3

Mean squared errors (MSEs) of multi-step ahead forecasts for the period of 100,000 years ago to 1000 years ago for the ice-age model (Castle and Hendry, 2020), score-driven homoskedastic t ice-age model (Blazsek and Escribano, 2022), and score-driven threshold ice-age model with two clusters using $Temp_t$.

	Ice-age model of Castle and Hendry (2020)	Score-driven ice-age model of Blazsek and Escribano (2022)	Score-driven threshold ice-age model, clustering for Ice_t , $CO_{2,t}$, and $Temp_t$	Score-driven threshold ice-age model, clustering for Ice_t and $CO_{2,t}$	Score-driven threshold ice-age model, clustering for Ice_t and $Temp_t$	Score-driven threshold ice-age model, clustering for $CO_{2,t}$ and $Temp_t$	Score-driven threshold ice-age model, clustering for Ice_t	Score-driven threshold ice-age model, clustering for $CO_{2,t}$	Score-driven threshold ice-age model, clustering for $Temp_t$
	MSE	MSE	MSE	MSE	MSE	MSE	MSE	MSE	MSE
Ice_t									
last 100000 years	0.0917	0.0969	0.0598	0.0648	0.0598	0.0766	0.0523	0.0705	0.0596
last 90000 years	0.1003	0.1058	0.0628	0.0686	0.0628	0.0816	0.0551	0.0742	0.0623
last 80000 years	0.1081	0.1148	0.0637	0.0686	0.0637	0.0782	0.0526	0.0791	0.0671
last 70000 years	0.1186	0.1258	0.0687	0.0759	0.0687	0.0842	0.0577	0.0871	0.0656
last 60000 years	0.1259	0.1317	0.0740	0.0838	0.0740	0.0895	0.0640	0.0951	0.0595
last 50000 years	0.1416	0.1472	0.0833	0.0915	0.0833	0.1029	0.0729	0.1030	0.0605
last 40000 years	0.1712	0.1765	0.1023	0.1122	0.1023	0.1255	0.0899	0.1264	0.0737
last 30000 years	0.2148	0.2134	0.1325	0.1474	0.1325	0.1607	0.1186	0.1662	0.0953
last 20000 years	0.3049	0.2911	0.1965	0.2182	0.1965	0.2383	0.1740	0.2454	0.1360
last 10000 years	0.4889	0.4527	0.3043	0.3524	0.3043	0.3732	0.2636	0.3887	0.1627
$CO_{2,t}$									
last 100000 years	0.0399	0.0424	0.0287	0.0331	0.0287	0.0312	0.0384	0.0206	0.0203
last 90000 years	0.0440	0.0470	0.0308	0.0363	0.0308	0.0338	0.0424	0.0224	0.0223
last 80000 years	0.0460	0.0494	0.0290	0.0354	0.0290	0.0300	0.0430	0.0217	0.0231
last 70000 years	0.0513	0.0552	0.0318	0.0399	0.0318	0.0330	0.0484	0.0245	0.0236
last 60000 years	0.0590	0.0634	0.0355	0.0457	0.0355	0.0371	0.0538	0.0278	0.0263
last 50000 years	0.0692	0.0746	0.0407	0.0529	0.0407	0.0405	0.0626	0.0315	0.0302
last 40000 years	0.0842	0.0902	0.0465	0.0635	0.0465	0.0465	0.0749	0.0364	0.0357
last 30000 years	0.1104	0.1165	0.0550	0.0817	0.0550	0.0574	0.0980	0.0454	0.0457
last 20000 years	0.1269	0.1224	0.0670	0.1041	0.0670	0.0726	0.1008	0.0576	0.0399
last 10000 years	0.1891	0.1733	0.0954	0.1548	0.0954	0.1055	0.1276	0.0835	0.0232
$Temp_t$									
last 100000 years	4.1809	4.5168	2.1591	3.2180	2.1591	2.6635	3.5485	2.3664	1.8878
last 90000 years	4.4536	4.8533	1.8784	3.3024	1.8784	2.4976	3.6959	2.3339	1.9771
last 80000 years	4.5747	5.0628	1.6850	3.1170	1.6850	1.8404	3.5842	2.2398	2.1104
last 70000 years	5.0599	5.6177	1.7345	3.3472	1.7345	1.9755	3.8953	2.3890	2.2622
last 60000 years	5.7960	6.4482	1.8759	3.7591	1.8759	2.1604	4.2985	2.6119	2.5300
last 50000 years	6.4533	7.2948	2.1204	3.9418	2.1204	2.4787	4.9986	2.5043	2.7074
last 40000 years	7.3939	8.1927	2.4885	4.7341	2.4885	2.9774	5.7713	2.9031	3.0469
last 30000 years	8.8750	9.3292	3.0859	6.0600	3.0859	3.7412	7.2605	3.5894	3.5919
last 20000 years	10.0692	9.5685	3.4864	7.6342	3.4864	4.6083	7.4055	4.3769	2.8362
last 10000 years	14.0302	12.8303	3.8247	9.4035	3.8247	5.5465	8.4037	5.0836	0.5984

dummy variables, which may represent clustering with respect to any of the subsets of Ice_t , $CO_{2,t}$, and $Temp_t$. We formulate the following score-driven threshold ice-age model:

$$y_t = \mu_t + v_t \tag{20}$$

$$\begin{aligned} \mu_t = & \gamma_0(1)D_{1,t} + \gamma_0(2)D_{2,t} + \gamma_0(3)D_{3,t} + [\Gamma_1(1)D_{1,t} + \Gamma_1(2)D_{2,t} \\ & + \Gamma_1(3)D_{3,t}]\mu_{t-1} + [\Gamma_2(1)D_{1,t} + \Gamma_2(2)D_{2,t} + \Gamma_2(3)D_{3,t}]z_t \\ & + [\Gamma_3(1)D_{1,t} + \Gamma_3(2)D_{2,t} + \Gamma_3(3)D_{3,t}]z_{t-1} \\ & + [\Psi(1)D_{1,t} + \Psi(2)D_{2,t} + \Psi(3)D_{3,t}]\mu_{t-1} \end{aligned} \tag{21}$$

$$\begin{aligned} v_t \sim & t_3[0, \Omega(1)\Omega(1)'D_{1,t} \\ & + \Omega(2)\Omega(2)'D_{2,t} + \Omega(3)\Omega(3)'D_{3,t}, v(1)D_{1,t} + v(2)D_{2,t} + v(3)D_{3,t}] \end{aligned} \tag{22}$$

for $t = 1, \dots, T$. The definitions of the variables and parameters and the methods of statistical inference coincide with those for the score-driven ice-age model of Section 3.1.

In Tables A.1, A.2, and A.3 of the Appendix, by using the estimation window for the period of 798,000 years ago to 1000 years ago, we present the parameter estimates and diagnostic test results for the score-driven threshold ice-age model, for which two clusters are defined using: (i) Ice_t and $CO_{2,t}$ for Table A.1, (ii) $CO_{2,t}$ and $Temp_t$ for Table A.2, and (iii) Ice_t , $CO_{2,t}$, and $Temp_t$ for Table A.3. We use these subsets of clustering variables, because they provide superior forecasting performances for the last 100,000 years, i.e., the specification of

Table A.1 provides the most accurate forecasts for Ice_t , the specification of Table A.2 provides the most accurate forecasts for $CO_{2,t}$, and the specification of Table A.3 provides the most accurate forecasts for $Temp_t$ (see more on this later in this section for the forecasting results). The C_1 , C_2 , and C_3 statistics indicate that y_t is covariance stationary for the three clusters. The LB tests for v_t and u_t indicate that each element of those vectors forms an independent time series. These diagnostic tests support the score-driven threshold ice-age model specifications of Table A.1, A2, and A3. We note that, for some alternative specifications of three clusters, the LB test does not support the independence of v_t and u_t .

In Fig. 6, by using the estimation window for the period of 798,000 years ago to 1000 years ago, we present the clusters which are used in the models of Table A.1, A2, A3; hence, (i) Ice_t is clustered with respect to Ice_t and $CO_{2,t}$ (Fig. 6(a)), (ii) $CO_{2,t}$ is clustered with respect to $CO_{2,t}$ and $Temp_t$ (Fig. 6(b)), and (iii) $Temp_t$ is clustered with respect to Ice_t , $CO_{2,t}$, and $Temp_t$ (Fig. 6(c)). For all these clustering methods, the dummies can be interpreted as follows: (i) $(D_{1,t}, D_{2,t}, D_{3,t}) = (1, 0, 0)$ indicates a regime with high level of Ice_t , low level of $CO_{2,t}$, and low level of $Temp_t$. (ii) $(D_{1,t}, D_{2,t}, D_{3,t}) = (0, 1, 0)$ indicates a regime with average level of Ice_t , average level of $CO_{2,t}$, and average level of $Temp_t$. (iii) $(D_{1,t}, D_{2,t}, D_{3,t}) = (0, 0, 1)$ indicates a regime with low level of Ice_t , high level of $CO_{2,t}$, and high level of $Temp_t$. We note that for the most recent regime, $D_{1,t} = 0$, $D_{2,t} = 0$, and $D_{3,t} = 1$ are observed, i.e., high level of global temperature, which started approximately 12,000 years ago.

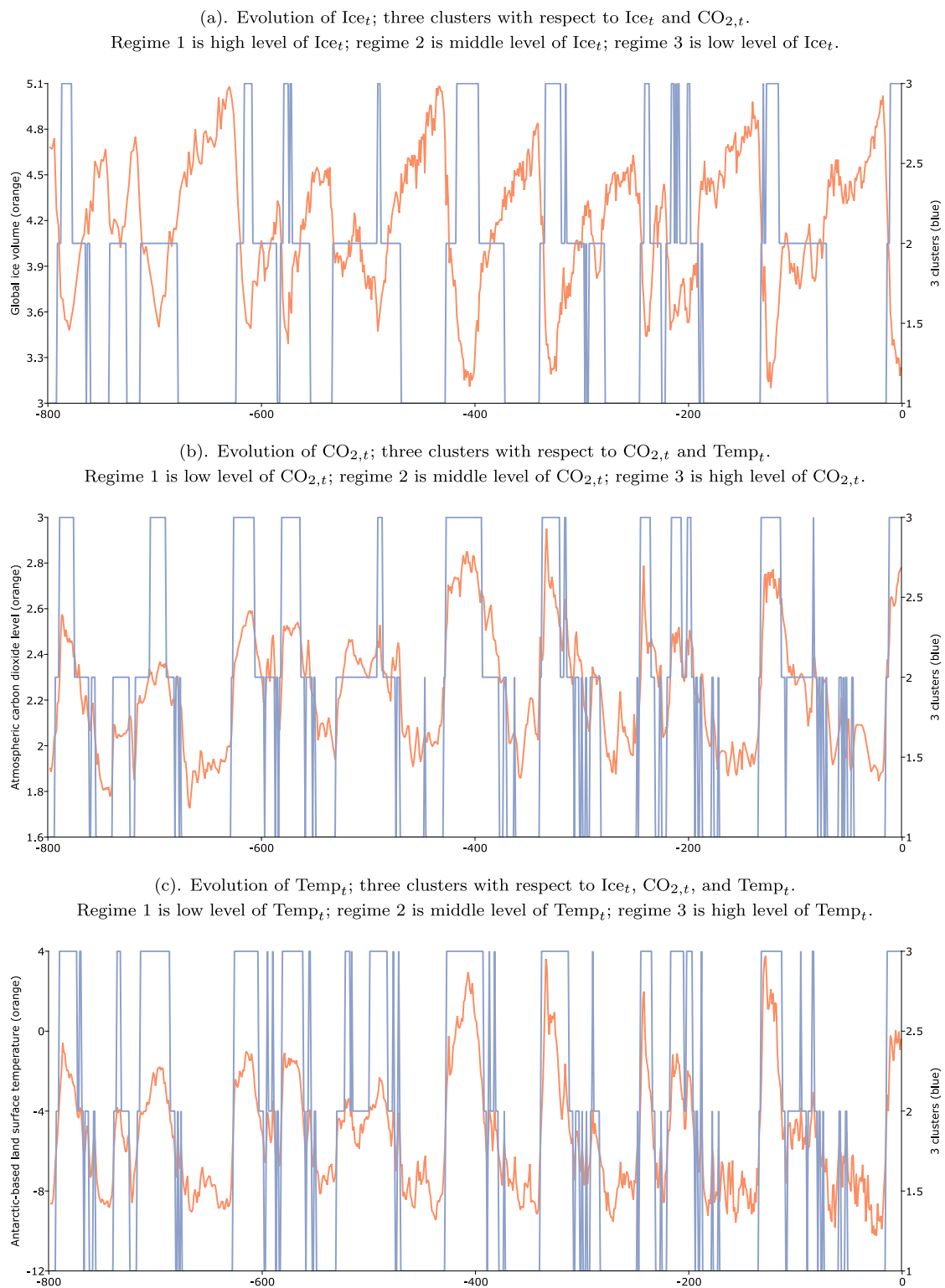


Fig. 6. Ward’s linkage clustering for three clusters with respect to the best-performing clustering method for each climate variable from Table 4. Note: We do not report cut-points, because clustering is done by using more than one variable for each panel.

Motivated by the work of Harvey (2013, p. 56), by comparing the likelihood-based model selection metrics of the score-driven threshold ice-age model using two clusters (Table 2(b)) and three clusters (Table A.1, A2, and A3), for almost all likelihood-based model selection metrics, for the estimation window for the period of 798,000 years ago to 1000 years ago, we find that the log-likelihood (LL) estimate

is higher for three clusters than for two clusters, and the Akaike information criterion (AIC), Bayesian information criterion (BIC), and Hannan–Quinn criterion (HQC) estimates are lower for three clusters than for two clusters. The results indicate that for the score-driven threshold ice-age model it is better to use three clusters rather than two.

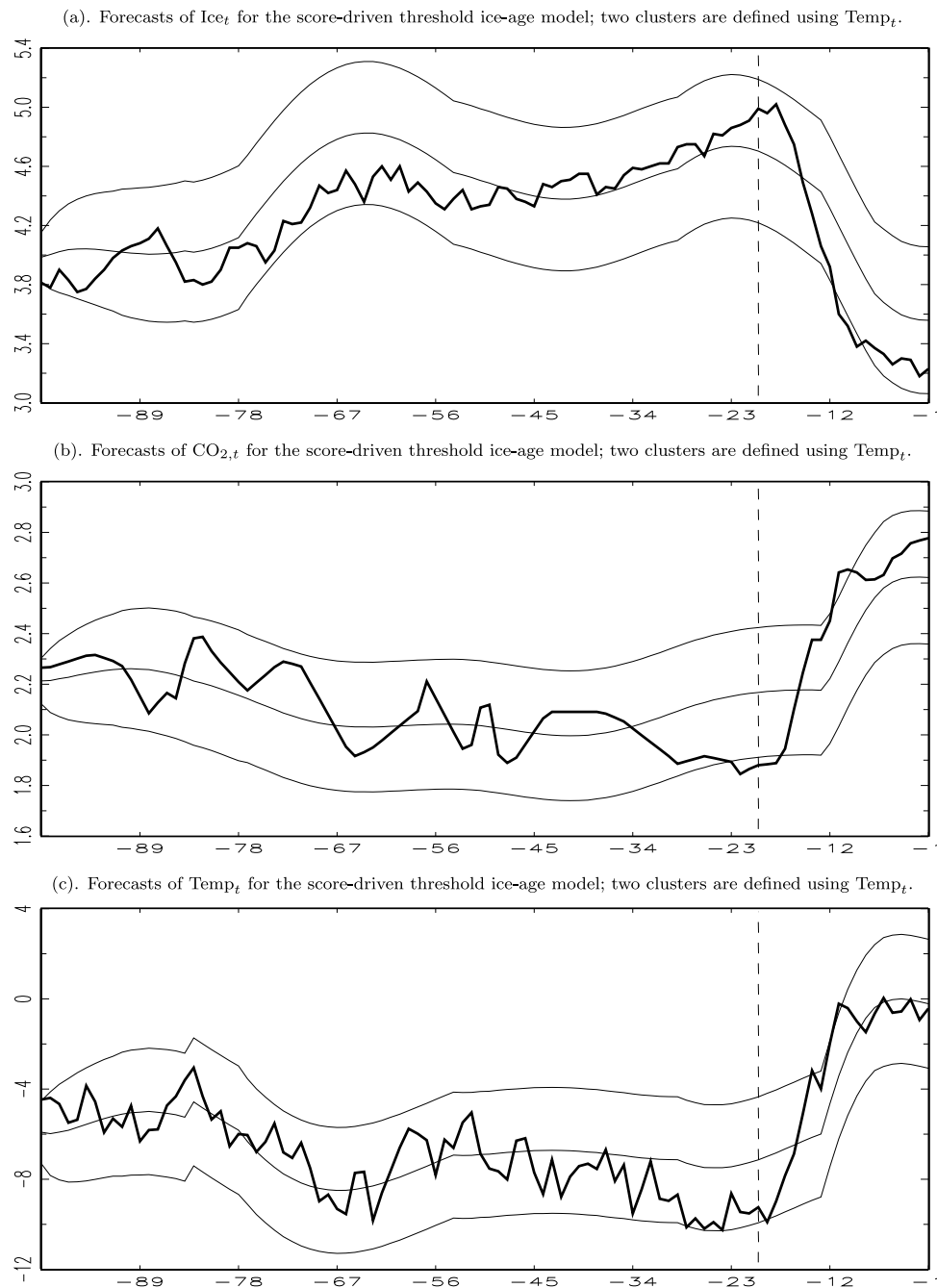


Fig. 7. Multi-step ahead forecasts of Ice_t , $CO_{2,t}$, and $Temp_t$ from 100,000 years ago to 1000 years ago, by using the best-performing score-driven threshold ice-age model with two clusters from [Table 3](#). *Note:* The confidence interval is ± 2 standard deviations of the forecasts. The best-performing model for two clusters for the forecasting of the last 20,000 years uses $Temp_t$ for clustering for all climate variables ([Table 3](#)). The dashed lines indicate 20,000 years ago.

3.4. Forecasting results

In [Tables 3](#) and [4](#), the multi-step ahead forecasting performances for Ice_t , $CO_{2,t}$, and $Temp_t$ are compared, for which the estimation window is for the period of 798,000 years ago to 101,000 years ago ($T = 698$) and the multi-step ahead forecasting window is for the period of the last 100,000 years ($T_f = 100$). We use the mean square error (MSE) loss function for performance evaluation. We note that similar forecasting performance results are obtained for the mean absolute error (MAE) loss function; those estimates are not reported here, but are available from the authors upon request. The loss function is averaged for different periods of the last 100,000 years (see [Tables 3](#) and [4](#)).

In [Table 3](#), by using the estimation window for the period of 798,000 years ago to 101,000 years ago, the forecasting results compare the ice-age models of [Castle and Hendry \(2020\)](#) and [Blazsek and Escribano \(2022\)](#) with the score-driven threshold ice-age model for all alternative clustering methods using two clusters. The results indicate that the forecasting accuracies of the score-driven threshold ice-age models dominate the forecasting accuracies of the ice-age models of [Castle and Hendry \(2020\)](#) and [Blazsek and Escribano \(2022\)](#). For most of the cases, the MSE results indicate that the score-driven threshold ice-age model using $Temp_t$ for clustering has the most accurate forecasting performance. Moreover, we also find that the forecasting performance of the score-driven threshold ice-age model using clustering for $Temp_t$ is superior to all alternatives in [Table 3](#) for the last 20,000 years of the historical sample period.

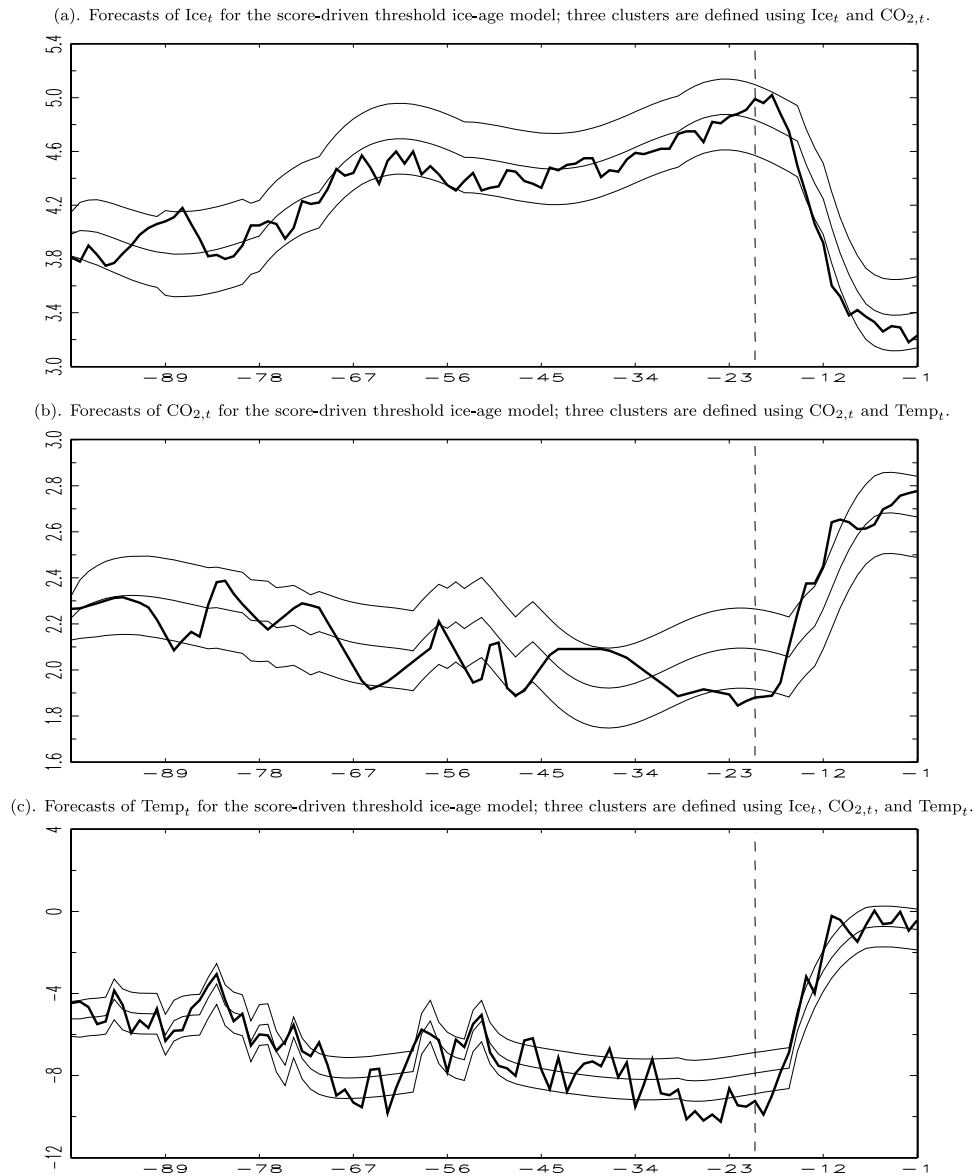


Fig. 8. Multi-step ahead forecasts of Ice_t , $CO_{2,t}$, and $Temp_t$ from 100,000 years ago to 1000 years ago, by using the best-performing score-driven threshold ice-age models for three clusters from Table 4. Note: The confidence interval is ± 2 standard deviations of the forecasts. Notice an increasing forecasting precision for all climate variables: (i) The true values are closer to the forecasts than in Fig. 7. (ii) The forecast intervals are narrower than in Fig. 7. The dashed lines indicate 20,000 years ago.

In Fig. 7, we present the multi-step ahead forecasts of the climate variables for the last 100,000 years of the sample period, by using the estimation window for the period of 798,000 years ago to 101,000 years ago, for score-driven threshold ice-age model by using $Temp_t$ in order to define two clusters. The results indicate that the forecasting precision of the score-driven threshold ice-age model using clustering for $Temp_t$ is superior to that of the ice-age model of Castle and Hendry (2020, p. 111).

In Table 4, by using the estimation window for the period of 798,000 years ago to 101,000 years ago, the forecasting results compare the score-driven threshold ice-age models for all alternative clustering methods, using three clusters. The results support the best-performing specifications from Table A.1, A2, and A3, and Fig. 6. Moreover, by comparing Tables 3 and 4 we find that the estimates of the forecasting performances of the score-driven threshold ice-age models using three clusters (Table 4) are superior to those of the score-driven threshold ice-age models using two clusters (Table 3).

In Fig. 8, we present the multi-step ahead forecasts of the climate variables for the last 100,000 years of the sample period, by using the estimation window for the period of 798,000 years ago to 101,000 years ago, for the best-performing score-driven threshold ice-age model using three clusters: (i) Ice_t is clustered with respect to Ice_t and $CO_{2,t}$ (Fig. 8(a)), (ii) $CO_{2,t}$ is clustered with respect to $CO_{2,t}$ and $Temp_t$ (Fig. 8(b)), and (iii) $Temp_t$ is clustered with respect to Ice_t , $CO_{2,t}$, and $Temp_t$ (Fig. 8(c)). We find an increasing forecasting precision for all climate variables, because the true values of the climate variables are closer to their forecasts in Fig. 8 than in Fig. 7. We also find that the forecast intervals are narrower in Fig. 8 than in Fig. 7.

Finally, we use the best-performing score-driven threshold ice-age models, using two and three clusters to forecast the climate variables for the forthcoming 5000 years, by using the estimation window for the period of 798,000 years ago to 1000 years ago. Due to the 1,000-year observation frequency, those forecasting results can be interpreted as benchmarks, which would have happened if humanity had not

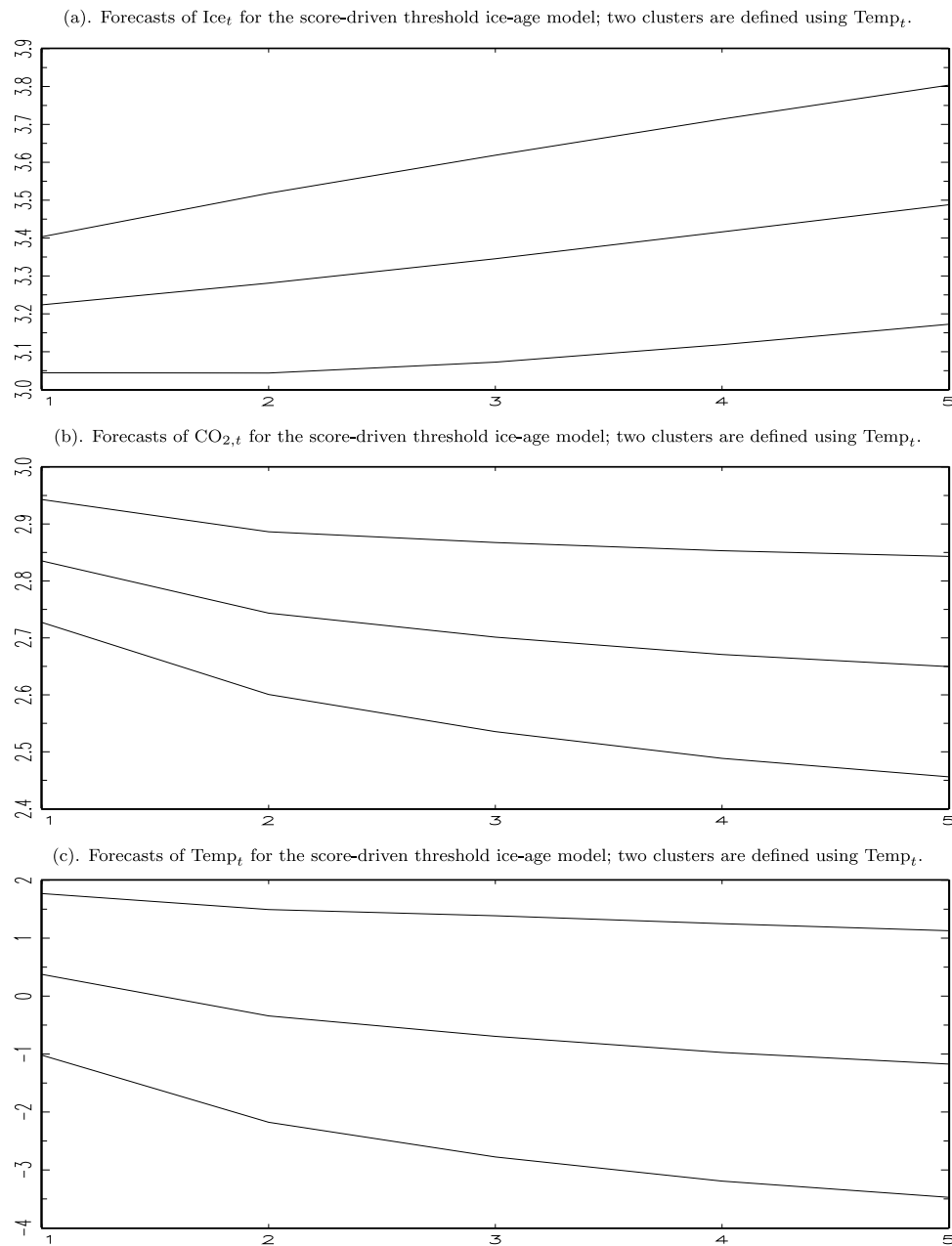


Fig. 9. Multi-step ahead out-of-sample forecasts of Ice_t , $CO_{2,t}$, and $Temp_t$ for the forthcoming 5000 years, by using the best-performing score-driven ice-age model with structural changes with two clusters from Table 3. Note: The confidence interval is ± 2 standard deviations of the forecasts. The best-performing model for two clusters for the forecasting of the last 20,000 years uses $Temp_t$ for clustering of all climate variables (Table 3).

burned fossil fuels since the Industrial Revolution. The corresponding multi-step ahead out-of-sample forecasts are presented in Figs. 9 and 10, respectively. These figures use the same model specifications for forecasting as Figs. 7 and 8, respectively. For the forecasting formulas of Figs. 9 and 10, we assume that the last regime of the historical sample period will continue for the forthcoming 5000 years, i.e., $D_{1,t} = 0$ and $D_{2,t} = 1$ (Fig. 9), and $D_{1,t} = 0$, $D_{2,t} = 0$, and $D_{3,t} = 1$ (Fig. 10), which are low level of Ice_t , high level of $CO_{2,t}$, and high level of $Temp_t$ for both figures. For the forthcoming 5,000 year period this is the most realistic assumption on the climate regime. For the purpose of robustness analysis, we also performed the same forecasting exercise of the less realistic case of $D_{1,t} = 0$, $D_{2,t} = 1$, and $D_{3,t} = 0$ which is average level of Ice_t , average level of $CO_{2,t}$, and average level of $Temp_t$, and the unrealistic case of $D_{1,t} = 1$, $D_{2,t} = 0$, and $D_{3,t} = 0$ which is high level of Ice_t , low level of $CO_{2,t}$, and low level of $Temp_t$. The forecasts of the climate variables for the forthcoming 5000 years for those alternatives

are practically identical to the forecasts of Figs. 9 and 10. Hence, the forecasting results of Figs. 9 and 10 are robust predictions of the climate variables.

By comparing Figs. 9 and 10, we find that the forecasting intervals for Ice_t and $Temp_t$ are clearly narrower in Fig. 10 than in Fig. 9. Moreover, we also find that the forecasting interval for $CO_{2,t}$ is slightly narrower in Fig. 10 than in Fig. 9. Hence, we find that the forecasting accuracy of the score-driven threshold ice-age models using three clusters is superior to the forecasting accuracy of the score-driven threshold ice-age models using two clusters. Both Figs. 9 and 10 show increasing global ice volume Ice_t , decreasing atmospheric $CO_{2,t}$ volume, and decreasing Antarctic land surface temperature $Temp_t$ for the next 5000 years. This indicates a turning point in the climate variables for the forthcoming 5000 years, under the assumption that humanity has not influenced significantly Earth's climate during the last 250 years.

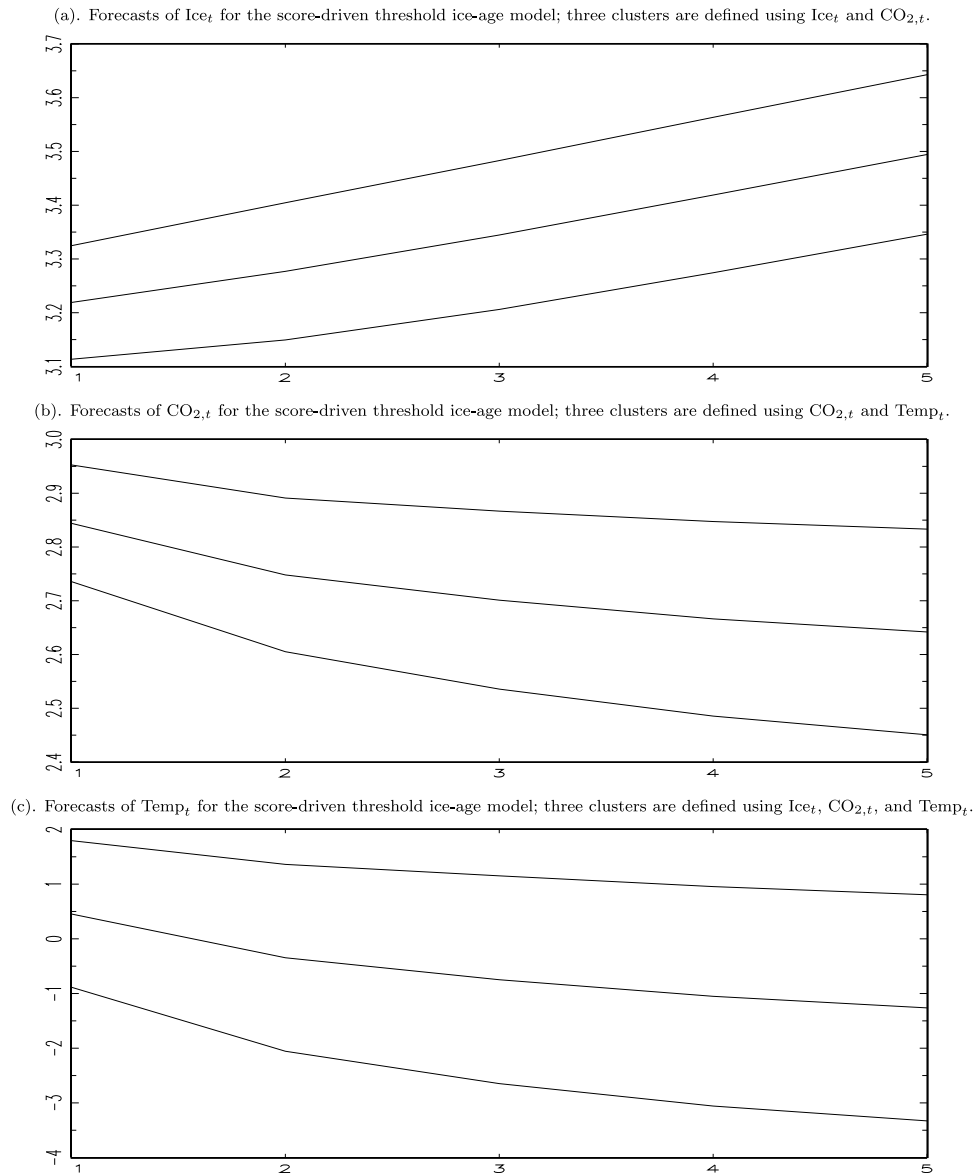


Fig. 10. Multi-step ahead out-of-sample forecasts of Ice_t , $CO_{2,t}$, and $Temp_t$ for the forthcoming 5000 years, by using the best-performing score-driven threshold ice-age models for three clusters from Table 4. Note: The confidence interval is ± 2 standard deviations of the forecasts. Notice an increasing forecasting precision: (i) The forecast intervals for Ice_t and $Temp_t$ are clearly narrower than in Fig. 9. (ii) The forecast interval for $CO_{2,t}$ is slightly narrower than in Fig. 9.

4. Conclusions

In the recent work of Blazsek and Escribano (2022), it is shown that the statistical performance of score-driven ice-age models is superior to that of the ice-age model of Castle and Hendry (2020), without using any sort of intervention analysis (i.e., impulse saturation variables), and it is also shown that the score-driven ice-age models are able to solve previous dynamic misspecifications. However, Blazsek and Escribano (2022) also show that the forecasting performances of both models are similar and none of those models are able to anticipate well the climate variables for the last 10,000 to 15,000 years. Motivated by this result, in this paper, we introduce new regime-switching score-driven ice-age models to capture the abrupt changes observed when climate variables exceed certain threshold values.

First, we have considered a score-driven Markov-switching ice-age model and we provided empirical evidence of having structural changes in our three climate variables. In particular, we have found clear asymmetric cyclical reactions during low-persistence periods of rapid increases in CO_2 and temperature versus the other regime of high-persistence periods with decreasing CO_2 and temperature. Furthermore,

we have also identified alternative regime switching periods by using temporal clusters built on high levels of one, two, or three of our climate variables. We have used Ward's clustering method and we have named our models score-driven threshold ice-age models. Estimation and forecasting results have supported the use of those models, since we have been able to anticipate well the evolution of the climate variables for the last 10,000 to 15,000 years. We have suggested using the optimal clustering which might be different for each of the three climate variables. Finally, by using the best-performing score-driven threshold ice-age models, we have provided out-of-sample forecasts of the climate variables for the forthcoming 5000 years. Without considering the extreme climate effects of the most recent 250 years of fossil fuels burned by humanity, we have identified the existence of synchronous turning points in the long-run cyclical evolution of the three climate variables, moving to a new period of increasing global ice volume, decreasing atmospheric CO_2 volume, and decreasing Antarctic land surface temperature in the next 5000 years. These long-run forecasting results may be used as a benchmark for comparisons with the forecasts of researchers who use more recent and more frequently observed data

Table 4

Mean squared errors (MSEs) of multi-step ahead forecasts for the period of 100,000 years ago to 1000 years ago for the score-driven threshold ice-age models with three clusters.

	Score-driven threshold ice-age model, clustering for Ice _t , CO _{2,t} , and Temp _t	Score-driven threshold ice-age model, clustering for Ice _t and CO _{2,t}	Score-driven threshold ice-age model, clustering for Ice _t and Temp _t	Score-driven threshold ice-age model, clustering for CO _{2,t} and Temp _t	Score-driven threshold ice-age model, clustering for Ice _t	Score-driven threshold ice-age model, clustering for CO _{2,t}	Score-driven threshold ice-age model, clustering for Temp _t
Ice _t	MSE	MSE	MSE	MSE	MSE	MSE	MSE
last 100000 years	0.0466	0.0255	0.0469	0.0504	0.0735	0.0696	0.0430
last 90000 years	0.0496	0.0255	0.0499	0.0536	0.0336	0.0755	0.0448
last 80000 years	0.0515	0.0241	0.0515	0.0514	0.0314	0.0793	0.0473
last 70000 years	0.0535	0.0259	0.0535	0.0539	0.0343	0.0864	0.0512
last 60000 years	0.0538	0.0264	0.0540	0.0530	0.0388	0.0947	0.0519
last 50000 years	0.0570	0.0231	0.0575	0.0575	0.0446	0.1057	0.0578
last 40000 years	0.0693	0.0266	0.0701	0.0703	0.0546	0.1300	0.0704
last 30000 years	0.0899	0.0331	0.0912	0.0916	0.0717	0.1714	0.0901
last 20000 years	0.1330	0.0466	0.1352	0.1357	0.1024	0.2541	0.1335
last 10000 years	0.1851	0.0339	0.1900	0.1468	0.1306	0.4160	0.1503
CO _{2,t}	MSE	MSE	MSE	MSE	MSE	MSE	MSE
last 100000 years	0.0176	0.0183	0.0179	0.0166	1.3852	0.0234	0.0174
last 90000 years	0.0195	0.0201	0.0198	0.0184	0.0720	0.0251	0.0191
last 80000 years	0.0207	0.0184	0.0208	0.0185	0.0568	0.0245	0.0201
last 70000 years	0.0219	0.0203	0.0219	0.0204	0.0521	0.0277	0.0228
last 60000 years	0.0241	0.0229	0.0242	0.0213	0.0499	0.0319	0.0230
last 50000 years	0.0263	0.0253	0.0264	0.0214	0.0553	0.0362	0.0240
last 40000 years	0.0286	0.0290	0.0288	0.0228	0.0651	0.0422	0.0257
last 30000 years	0.0315	0.0359	0.0319	0.0254	0.0846	0.0526	0.0296
last 20000 years	0.0328	0.0349	0.0334	0.0224	0.0744	0.0714	0.0247
last 10000 years	0.0360	0.0204	0.0378	0.0090	0.0689	0.1049	0.0099
Temp _t	MSE	MSE	MSE	MSE	MSE	MSE	MSE
last 100000 years	0.8043	2.2282	0.8109	1.0177	24.3943	2.5421	1.0812
last 90000 years	0.8537	2.2020	0.8590	1.0409	10.5759	2.5202	1.1254
last 80000 years	0.9318	1.9131	0.9363	1.0560	4.5172	2.4398	1.1783
last 70000 years	0.9917	1.9628	0.9898	1.1895	3.9975	2.6847	1.1633
last 60000 years	1.0044	2.1460	1.0127	1.1916	3.9305	2.9893	1.1782
last 50000 years	1.1187	1.9586	1.1273	1.3304	4.6014	3.0771	1.3067
last 40000 years	1.2364	2.2527	1.2470	1.5603	5.3153	3.6479	1.5533
last 30000 years	1.4140	2.7468	1.4306	1.8421	6.6035	4.6595	1.8770
last 20000 years	0.9833	2.6371	1.0227	1.6540	5.8365	6.1343	1.6439
last 10000 years	0.3574	0.4236	0.4307	0.9056	4.4157	7.4776	0.9700

Table A.1

Score-driven threshold ice-age model with three clusters which provides the most accurate forecasts of Ice_t (Table 4) for the period of 798,000 to 1000 years ago.

Score-driven threshold ice-age model with clustering with respect to Ice_t and CO_{2,t}
 Regime 1 = high Ice_t and low CO_{2,t}; regime 2 = middle Ice_t and CO_{2,t}; regime 3 = low Ice_t and high CO_{2,t}

$\gamma_{0,1}(1)$	1.4277*** (0.4542)	$\gamma_{0,1}(2)$	1.2157** (0.5742)	$\gamma_{0,1}(3)$	3.1102*** (0.8325)	C ₁	0.8842
$\gamma_{0,2}(1)$	1.4277** (0.6434)	$\gamma_{0,2}(2)$	2.1594*** (0.5851)	$\gamma_{0,2}(3)$	4.4886*** (1.4178)	C ₂	0.8425
$\gamma_{0,3}(1)$	-1.9481 (1.7411)	$\gamma_{0,3}(2)$	0.4278 (1.2814)	$\gamma_{0,3}(3)$	6.6513+ (4.1852)	C ₃	0.6987
$\Gamma_{1,1,1}(1)$	0.8842*** (0.0270)	$\Gamma_{1,1,1}(2)$	0.7524*** (0.0286)	$\Gamma_{1,1,1}(3)$	0.6325*** (0.0486)	LB $u_{1,t}$	21.3765 (0.8093)
$\Gamma_{1,1,3}(1)$	0.0005 (0.0053)	$\Gamma_{1,1,3}(2)$	-0.0073* (0.0040)	$\Gamma_{1,1,3}(3)$	-0.0222*** (0.0055)	LB $u_{2,t}$	34.4545 (0.1863)
$\Gamma_{1,2,2}(1)$	0.7157*** (0.0437)	$\Gamma_{1,2,2}(2)$	0.7946*** (0.0415)	$\Gamma_{1,2,2}(3)$	0.4893*** (0.1290)	LB $u_{3,t}$	28.6976 (0.4280)
$\Gamma_{1,2,3}(1)$	0.0220*** (0.0055)	$\Gamma_{1,2,3}(2)$	0.0131*** (0.0041)	$\Gamma_{1,2,3}(3)$	0.0294*** (0.0086)	LB $u_{1,t}$	24.2263 (0.6695)
$\Gamma_{1,3,2}(1)$	0.1311 (0.6347)	$\Gamma_{1,3,2}(2)$	-0.4361 (0.4632)	$\Gamma_{1,3,2}(3)$	-2.4115+ (1.5197)	LB $u_{2,t}$	29.8172 (0.3720)
$\Gamma_{1,3,3}(1)$	0.7864*** (0.0722)	$\Gamma_{1,3,3}(2)$	0.8860*** (0.0435)	$\Gamma_{1,3,3}(3)$	0.8527*** (0.1063)	LB $u_{3,t}$	31.5100 (0.2949)
$\Gamma_{2,1,1}(1)$	70.0455 (55.8945)	$\Gamma_{2,1,1}(2)$	42.1530 (44.7704)	$\Gamma_{2,1,1}(3)$	-124.7862 (116.7117)	LL	1.7830
$\Gamma_{2,1,4}(1)$	-34.6457* (23.5207)	$\Gamma_{2,1,4}(2)$	-31.6182* (17.7643)	$\Gamma_{2,1,4}(3)$	57.1456 (50.5386)	AIC	-3.2879
$\Gamma_{2,1,5}(1)$	-5.4665** (2.1688)	$\Gamma_{2,1,5}(2)$	-5.8799*** (1.3888)	$\Gamma_{2,1,5}(3)$	-2.7563+ (1.7315)	BIC	-2.6366
$\Gamma_{2,2,1}(1)$	18.2079*** (5.8146)	$\Gamma_{2,2,1}(2)$	14.1910+ (9.1732)	$\Gamma_{2,2,1}(3)$	-30.1201* (16.9529)	HQC	-3.0376
$\Gamma_{2,2,8}(1)$	0.1656* (0.0925)	$\Gamma_{2,2,8}(2)$	0.2388*** (0.0832)	$\Gamma_{2,2,8}(3)$	0.6516*** (0.2409)		
$\Gamma_{2,3,1}(1)$	-279.7774*** (74.3145)	$\Gamma_{2,3,1}(2)$	-321.0749*** (62.1935)	$\Gamma_{2,3,1}(3)$	-189.3791 (137.5875)		
$\Gamma_{2,3,4}(1)$	201.2026*** (42.3791)	$\Gamma_{2,3,4}(2)$	303.3058*** (52.9524)	$\Gamma_{2,3,4}(3)$	64.4725 (105.3050)		
$\Gamma_{2,3,5}(1)$	32.3395* (17.6699)	$\Gamma_{2,3,5}(2)$	29.9243*** (9.2833)	$\Gamma_{2,3,5}(3)$	41.7598*** (13.2628)		
$\Gamma_{3,1,1}(1)$	-73.4795 (55.1368)	$\Gamma_{3,1,1}(2)$	-10.6816 (51.8357)	$\Gamma_{3,1,1}(3)$	114.7731 (133.7364)		
$\Gamma_{3,1,2}(1)$	-0.3783** (0.1691)	$\Gamma_{3,1,2}(2)$	-0.0989 (0.2397)	$\Gamma_{3,1,2}(3)$	-0.7981** (0.3303)		
$\Gamma_{3,1,4}(1)$	36.4495+ (23.4059)	$\Gamma_{3,1,4}(2)$	18.1064 (20.5495)	$\Gamma_{3,1,4}(3)$	-52.1673 (56.4184)		
$\Gamma_{3,2,1}(1)$	-51.1168*** (12.7793)	$\Gamma_{3,2,1}(2)$	-23.5842* (14.8972)	$\Gamma_{3,2,1}(3)$	55.4346** (27.2512)		
$\Gamma_{3,2,2}(1)$	-1.1129** (0.4541)	$\Gamma_{3,2,2}(2)$	-1.2507*** (0.4080)	$\Gamma_{3,2,2}(3)$	-2.8456** (1.1417)		
$\Gamma_{3,2,4}(1)$	13.9247*** (5.2111)	$\Gamma_{3,2,4}(2)$	4.0613 (3.8751)	$\Gamma_{3,2,4}(3)$	-11.1995* (7.4730)		
$\Gamma_{3,3,4}(1)$	-82.0721** (31.9618)	$\Gamma_{3,3,4}(2)$	-165.6717*** (44.3043)	$\Gamma_{3,3,4}(3)$	2.6060 (96.7154)		
$\Psi_{1,1,1}(1)$	0.7840*** (0.0664)	$\Psi_{1,1,1}(2)$	0.8733*** (0.0860)	$\Psi_{1,1,1}(3)$	1.0173*** (0.1613)		

(continued on next page)

Table A.1 (continued).

Score-driven threshold ice-age model with clustering with respect to Ice_t and $CO_{2,t}$
 Regime 1 = high Ice_t and low $CO_{2,t}$; regime 2 = middle Ice_t and $CO_{2,t}$; regime 3 = low Ice_t and high $CO_{2,t}$

$\Psi_{1,1,3}(1)$	-0.0229*** (0.0078)	$\Psi_{1,1,3}(2)$	-0.0225*** (0.0087)	$\Psi_{1,1,3}(3)$	-0.0727*** (0.0175)
$\Psi_{1,2,2}(1)$	1.3569*** (0.0776)	$\Psi_{1,2,2}(2)$	1.4874*** (0.0955)	$\Psi_{1,2,2}(3)$	0.9933*** (0.1829)
$\Psi_{1,2,3}(1)$	0.0169*** (0.0043)	$\Psi_{1,2,3}(2)$	0.0194*** (0.0057)	$\Psi_{1,2,3}(3)$	0.0121*** (0.0022)
$\Psi_{1,3,2}(1)$	3.7478*** (1.2826)	$\Psi_{1,3,2}(2)$	6.9428*** (1.2316)	$\Psi_{1,3,2}(3)$	1.2666 (2.2240)
$\Psi_{1,3,3}(1)$	0.8312*** (0.0731)	$\Psi_{1,3,3}(2)$	1.0423*** (0.0804)	$\Psi_{1,3,3}(3)$	2.5247*** (0.2118)
$\Omega_{2,1}(1)$	0.0819*** (0.0032)	$\Omega_{2,1}(2)$	0.0800*** (0.0034)	$\Omega_{2,1}(3)$	0.0523*** (0.0052)
$\Omega_{2,2}(1)$	-0.0070*** (0.0027)	$\Omega_{2,2}(2)$	-0.0075** (0.0030)	$\Omega_{2,2}(3)$	-0.0083 (0.0084)
$\Omega_{2,3}(1)$	0.0408*** (0.0015)	$\Omega_{2,3}(2)$	0.0480*** (0.0020)	$\Omega_{2,3}(3)$	0.0468*** (0.0058)
$\Omega_{3,1}(1)$	-0.1553*** (0.0462)	$\Omega_{3,1}(2)$	-0.0857** (0.0410)	$\Omega_{3,1}(3)$	-0.0480 (0.0819)
$\Omega_{3,2}(1)$	0.2604*** (0.0412)	$\Omega_{3,2}(2)$	0.3927*** (0.0404)	$\Omega_{3,2}(3)$	0.3164*** (0.0602)
$\Omega_{3,3}(1)$	0.6699*** (0.0256)	$\Omega_{3,3}(2)$	0.5835*** (0.0245)	$\Omega_{3,3}(3)$	0.4362*** (0.0460)
$\nu(1)$	3.5274*** (0.2063)	$\nu(2)$	3.1033*** (0.1755)	$\nu(3)$	1.8076*** (0.1757)

Note: $C_1 < 1$ is covariance stationarity of regime 1; $C_2 < 1$ is covariance stationarity of regime 2; $C_3 < 1$ is covariance stationarity of regime 3. The Ljung–Box (LB) statistics (p -values in parentheses) use the lag-order $\sqrt{T} \approx 28$. Log-likelihood (LL); Akaike information criterion (AIC); Bayesian information criterion (BIC); Hannan-Quinn criterion (HQC). Gradient-based standard errors are reported in parentheses.

*Parameter significance at the 15% level.

**Parameter significance at the 10% level.

***Parameter significance at the 5% level.

****Parameter significance at the 1% level.

Table A.2

Score-driven threshold ice-age model with three clusters which provides the most accurate forecasts of $CO_{2,t}$ (Table 4) for the period of 798,000 to 1000 years ago.

Score-driven threshold ice-age model with clustering with respect to $CO_{2,t}$ and $Temp_t$
 Regime 1 = low $Temp_t$, $CO_{2,t}$; regime 2 = middle $Temp_t$, $CO_{2,t}$; regime 3 = high $Temp_t$, $CO_{2,t}$

$\gamma_{0,1}(1)$	1.4169*** (0.3849)	$\gamma_{0,1}(2)$	0.8729* (0.6037)	$\gamma_{0,1}(3)$	2.9979*** (0.9448)	C_1	0.9633
$\gamma_{0,2}(1)$	1.4169*** (0.5773)	$\gamma_{0,2}(2)$	2.1366*** (0.6505)	$\gamma_{0,2}(3)$	3.7865*** (1.0300)	C_2	0.8162
$\gamma_{0,3}(1)$	-7.6029*** (1.4823)	$\gamma_{0,3}(2)$	-2.2624** (1.0791)	$\gamma_{0,3}(3)$	6.1613* (3.1907)	C_3	0.8323
$\Gamma_{1,1,1}(1)$	0.9633*** (0.0248)	$\Gamma_{1,1,1}(2)$	0.8162*** (0.0278)	$\Gamma_{1,1,1}(3)$	0.8323*** (0.0339)	LB $v_{1,t}$	18.5292 (0.9120)
$\Gamma_{1,1,3}(1)$	0.0147** (0.0060)	$\Gamma_{1,1,3}(2)$	-0.0177*** (0.0060)	$\Gamma_{1,1,3}(3)$	-0.0148** (0.0068)	LB $v_{2,t}$	31.7889 (0.2832)
$\Gamma_{1,2,2}(1)$	0.8017*** (0.0345)	$\Gamma_{1,2,2}(2)$	0.8104*** (0.0403)	$\Gamma_{1,2,2}(3)$	0.5245*** (0.0884)	LB $v_{3,t}$	36.2249 (0.1370)
$\Gamma_{1,2,3}(1)$	0.0146*** (0.0042)	$\Gamma_{1,2,3}(2)$	0.0040 (0.0041)	$\Gamma_{1,2,3}(3)$	0.0331*** (0.0083)	LB $u_{1,t}$	21.5846 (0.8001)
$\Gamma_{1,3,2}(1)$	1.2984*** (0.4932)	$\Gamma_{1,3,2}(2)$	-0.0377 (0.3915)	$\Gamma_{1,3,2}(3)$	-2.1979* (1.1425)	LB $u_{2,t}$	32.9488 (0.2376)
$\Gamma_{1,3,3}(1)$	0.3788*** (0.0727)	$\Gamma_{1,3,3}(2)$	0.5447*** (0.0512)	$\Gamma_{1,3,3}(3)$	0.9444*** (0.1049)	LB $u_{3,t}$	29.5934 (0.3829)
$\Gamma_{2,1,1}(1)$	28.5553 (46.3229)	$\Gamma_{2,1,1}(2)$	28.5553 (46.3229)	$\Gamma_{2,1,1}(3)$	-29.7489 (106.6205)	LL	1.9213
$\Gamma_{2,1,4}(1)$	-16.3650 (19.4494)	$\Gamma_{2,1,4}(2)$	-16.3650 (19.4494)	$\Gamma_{2,1,4}(3)$	1.0636 (44.6027)	AIC	-3.5643
$\Gamma_{2,1,5}(1)$	-4.5588*** (1.6229)	$\Gamma_{2,1,5}(2)$	-4.5588*** (1.6229)	$\Gamma_{2,1,5}(3)$	-4.8361** (2.0406)	BIC	-2.9131
$\Gamma_{2,2,1}(1)$	9.7223* (5.8362)	$\Gamma_{2,2,1}(2)$	9.7223* (5.8362)	$\Gamma_{2,2,1}(3)$	-0.9530 (17.6886)	HQC	-3.3141
$\Gamma_{2,2,8}(1)$	0.1615* (0.0863)	$\Gamma_{2,2,8}(2)$	0.1615* (0.0863)	$\Gamma_{2,2,8}(3)$	0.4144*** (0.1485)		
$\Gamma_{2,3,1}(1)$	-290.8906*** (67.4776)	$\Gamma_{2,3,1}(2)$	-290.8906*** (67.4776)	$\Gamma_{2,3,1}(3)$	-313.4403*** (106.2669)		
$\Gamma_{2,3,4}(1)$	103.7901** (41.7651)	$\Gamma_{2,3,4}(2)$	103.7901** (41.7651)	$\Gamma_{2,3,4}(3)$	233.3530** (102.1411)		
$\Gamma_{2,3,5}(1)$	26.9295* (15.7809)	$\Gamma_{2,3,5}(2)$	26.9295* (15.7809)	$\Gamma_{2,3,5}(3)$	15.9502 (12.6705)		
$\Gamma_{3,1,1}(1)$	-49.6861 (45.6694)	$\Gamma_{3,1,1}(2)$	-49.6861 (45.6694)	$\Gamma_{3,1,1}(3)$	10.9718 (118.8264)		
$\Gamma_{3,1,2}(1)$	-0.4798*** (0.1414)	$\Gamma_{3,1,2}(2)$	-0.4798*** (0.1414)	$\Gamma_{3,1,2}(3)$	-1.0341*** (0.3846)		
$\Gamma_{3,1,4}(1)$	25.6552 (19.2396)	$\Gamma_{3,1,4}(2)$	25.6552 (19.2396)	$\Gamma_{3,1,4}(3)$	7.6045 (49.0217)		
$\Gamma_{3,2,1}(1)$	-36.1261*** (11.9673)	$\Gamma_{3,2,1}(2)$	-36.1261*** (11.9673)	$\Gamma_{3,2,1}(3)$	-1.6609 (24.7657)		
$\Gamma_{3,2,2}(1)$	-1.0757** (0.4248)	$\Gamma_{3,2,2}(2)$	-1.0757** (0.4248)	$\Gamma_{3,2,2}(3)$	-2.0220*** (0.7342)		
$\Gamma_{3,2,4}(1)$	11.1919** (4.5159)	$\Gamma_{3,2,4}(2)$	11.1919** (4.5159)	$\Gamma_{3,2,4}(3)$	0.3632 (6.7152)		
$\Gamma_{3,3,4}(1)$	19.4779 (32.0427)	$\Gamma_{3,3,4}(2)$	19.4779 (32.0427)	$\Gamma_{3,3,4}(3)$	-109.9444 (97.0771)		
$\Psi_{1,1,1}(1)$	0.7537*** (0.0694)	$\Psi_{1,1,1}(2)$	0.9655*** (0.0817)	$\Psi_{1,1,1}(3)$	1.0149*** (0.1273)		
$\Psi_{1,1,3}(1)$	-0.0116 (0.0097)	$\Psi_{1,1,3}(2)$	-0.0117 (0.0125)	$\Psi_{1,1,3}(3)$	-0.0376** (0.0154)		
$\Psi_{1,2,2}(1)$	1.4896*** (0.0936)	$\Psi_{1,2,2}(2)$	1.5014*** (0.0983)	$\Psi_{1,2,2}(3)$	1.1020*** (0.1349)		
$\Psi_{1,2,3}(1)$	0.0110** (0.0052)	$\Psi_{1,2,3}(2)$	0.0016 (0.0069)	$\Psi_{1,2,3}(3)$	0.0059*** (0.0014)		
$\Psi_{1,3,2}(1)$	4.4487*** (1.1206)	$\Psi_{1,3,2}(2)$	3.4156*** (1.0317)	$\Psi_{1,3,2}(3)$	1.4002 (1.7893)		
$\Psi_{1,3,3}(1)$	0.5619*** (0.0676)	$\Psi_{1,3,3}(2)$	0.7642*** (0.0918)	$\Psi_{1,3,3}(3)$	1.4215*** (0.1638)		
$\Omega_{2,1}(1)$	0.0802*** (0.0035)	$\Omega_{2,1}(2)$	0.0778*** (0.0037)	$\Omega_{2,1}(3)$	0.0866*** (0.0050)		
$\Omega_{2,2}(1)$	-0.0048* (0.0025)	$\Omega_{2,2}(2)$	-0.0067*** (0.0031)	$\Omega_{2,2}(3)$	-0.0127** (0.0053)		
$\Omega_{2,3}(1)$	0.0382*** (0.0014)	$\Omega_{2,3}(2)$	0.0444*** (0.0019)	$\Omega_{2,3}(3)$	0.0507*** (0.0033)		
$\Omega_{3,1}(1)$	-0.0639* (0.0364)	$\Omega_{3,1}(2)$	-0.0610* (0.0382)	$\Omega_{3,1}(3)$	-0.1205** (0.0605)		
$\Omega_{3,2}(1)$	0.1475*** (0.0379)	$\Omega_{3,2}(2)$	0.2160*** (0.0366)	$\Omega_{3,2}(3)$	0.4018*** (0.0518)		
$\Omega_{3,3}(1)$	0.5430*** (0.0219)	$\Omega_{3,3}(2)$	0.5045*** (0.0271)	$\Omega_{3,3}(3)$	0.5248*** (0.0331)		
$\nu(1)$	3.3456*** (0.2150)	$\nu(2)$	3.1586*** (0.2537)	$\nu(3)$	2.7838*** (0.2407)		

Note: $C_1 < 1$ is covariance stationarity of regime 1; $C_2 < 1$ is covariance stationarity of regime 2; $C_3 < 1$ is covariance stationarity of regime 3. The Ljung–Box (LB) statistics (p -values in parentheses) use the lag-order $\sqrt{T} \approx 28$. Log-likelihood (LL); Akaike information criterion (AIC); Bayesian information criterion (BIC); Hannan-Quinn criterion (HQC). Gradient-based standard errors are reported in parentheses.

*Parameter significance at the 15% level.

**Parameter significance at the 10% level.

***Parameter significance at the 5% level.

****Parameter significance at the 1% level.

Table A.3

Score-driven threshold ice-age model with three clusters which provides the most accurate forecasts of Temp, (Table 4) for the period of 798,000 to 1000 years ago.

Score-driven threshold ice-age model with clustering with respect to Ice_t, CO_{2,t}, and Temp_t
 Regime 1 = high Ice_t, low Temp_t, and CO_{2,t}; regime 2 = middle Ice_t, Temp_t, and CO_{2,t}; regime 3 = low Ice_t, high Temp_t, and CO_{2,t}

$\gamma_{0,1}(1)$	1.0889*** (0.3594)	$\gamma_{0,1}(2)$	0.6614 (0.9558)	$\gamma_{0,1}(3)$	2.7643*** (0.7455)	C_1	0.9674
$\gamma_{0,2}(1)$	1.0889*** (0.5321)	$\gamma_{0,2}(2)$	2.6976*** (0.9024)	$\gamma_{0,2}(3)$	2.6669*** (0.7089)	C_2	0.8066
$\gamma_{0,3}(1)$	-6.8238*** (1.3727)	$\gamma_{0,3}(2)$	-2.9773*** (0.8022)	$\gamma_{0,3}(3)$	0.8206 (2.3245)	C_3	0.8389
$\Gamma_{1,1,1}(1)$	0.9674*** (0.0239)	$\Gamma_{1,1,1}(2)$	0.8053*** (0.0370)	$\Gamma_{1,1,1}(3)$	0.8389*** (0.0258)	LB $v_{1,t}$	20.2289 (0.8560)
$\Gamma_{1,1,3}(1)$	0.0100* (0.0056)	$\Gamma_{1,1,3}(2)$	-0.0184** (0.0091)	$\Gamma_{1,1,3}(3)$	-0.0135*** (0.0051)	LB $v_{2,t}$	29.9351 (0.3663)
$\Gamma_{1,2,2}(1)$	0.7930*** (0.0306)	$\Gamma_{1,2,2}(2)$	0.8060*** (0.0423)	$\Gamma_{1,2,2}(3)$	0.7300*** (0.0609)	LB $v_{3,t}$	18.0759 (0.9242)
$\Gamma_{1,2,3}(1)$	0.0174*** (0.0040)	$\Gamma_{1,2,3}(2)$	-0.0017 (0.0048)	$\Gamma_{1,2,3}(3)$	0.0159*** (0.0058)	LB $u_{1,t}$	19.0565 (0.8964)
$\Gamma_{1,3,2}(1)$	1.2116*** (0.4619)	$\Gamma_{1,3,2}(2)$	-0.1617 (0.2957)	$\Gamma_{1,3,2}(3)$	-0.3390 (0.8389)	LB $u_{2,t}$	31.8646 (0.2801)
$\Gamma_{1,3,3}(1)$	0.4466*** (0.0680)	$\Gamma_{1,3,3}(2)$	0.3410*** (0.0434)	$\Gamma_{1,3,3}(3)$	0.8048*** (0.0960)	LB $u_{3,t}$	21.0742 (0.8222)
$\Gamma_{2,1,1}(1)$	36.0145 (45.4817)	$\Gamma_{2,1,1}(2)$	76.7199* (50.5119)	$\Gamma_{2,1,1}(3)$	45.8113 (70.9087)	LL	1.9596
$\Gamma_{2,1,4}(1)$	-18.8903 (19.0435)	$\Gamma_{2,1,4}(2)$	-37.2693* (21.5833)	$\Gamma_{2,1,4}(3)$	-30.1589 (29.2719)	AIC	-3.6411
$\Gamma_{2,1,5}(1)$	-4.5857*** (1.5247)	$\Gamma_{2,1,5}(2)$	-5.8856*** (1.7520)	$\Gamma_{2,1,5}(3)$	-4.5873*** (1.6636)	BIC	-2.9898
$\Gamma_{2,2,1}(1)$	9.8492* (5.7035)	$\Gamma_{2,2,1}(2)$	19.1657* (10.2329)	$\Gamma_{2,2,1}(3)$	-2.3528 (13.5333)	HQC	-3.3909
$\Gamma_{2,2,8}(1)$	0.1667** (0.0827)	$\Gamma_{2,2,8}(2)$	0.2317* (0.1199)	$\Gamma_{2,2,8}(3)$	0.3432*** (0.1018)		
$\Gamma_{2,3,1}(1)$	-264.5521*** (64.6204)	$\Gamma_{2,3,1}(2)$	-115.9592** (48.6373)	$\Gamma_{2,3,1}(3)$	-355.4575*** (83.6406)		
$\Gamma_{2,3,4}(1)$	108.0166*** (41.1198)	$\Gamma_{2,3,4}(2)$	113.5697*** (43.5344)	$\Gamma_{2,3,4}(3)$	225.4502*** (83.5444)		
$\Gamma_{2,3,5}(1)$	32.2982** (15.6664)	$\Gamma_{2,3,5}(2)$	23.8292** (9.6551)	$\Gamma_{2,3,5}(3)$	16.2034* (10.2112)		
$\Gamma_{3,1,1}(1)$	-48.1296 (45.3757)	$\Gamma_{3,1,1}(2)$	-38.3228 (58.2920)	$\Gamma_{3,1,1}(3)$	-65.5521 (82.9802)		
$\Gamma_{3,1,2}(1)$	-0.3646*** (0.1347)	$\Gamma_{3,1,2}(2)$	0.0278 (0.4131)	$\Gamma_{3,1,2}(3)$	-0.9393*** (0.3092)		
$\Gamma_{3,1,4}(1)$	24.3584 (19.0105)	$\Gamma_{3,1,4}(2)$	20.8430 (24.7440)	$\Gamma_{3,1,4}(3)$	38.9456 (34.0419)		
$\Gamma_{3,2,1}(1)$	-31.6416*** (11.3099)	$\Gamma_{3,2,1}(2)$	-46.6994** (21.2248)	$\Gamma_{3,2,1}(3)$	0.1578 (18.6213)		
$\Gamma_{3,2,2}(1)$	-1.0745*** (0.3984)	$\Gamma_{3,2,2}(2)$	-1.5093** (0.6094)	$\Gamma_{3,2,2}(3)$	-1.6297*** (0.5003)		
$\Gamma_{3,2,4}(1)$	9.1421** (4.3105)	$\Gamma_{3,2,4}(2)$	11.7559* (7.4019)	$\Gamma_{3,2,4}(3)$	0.7905 (4.9049)		
$\Gamma_{3,3,4}(1)$	3.2870 (31.0725)	$\Gamma_{3,3,4}(2)$	-65.6671** (32.7232)	$\Gamma_{3,3,4}(3)$	-78.7713 (78.6988)		
$\Psi_{1,1,1}(1)$	0.8107*** (0.0674)	$\Psi_{1,1,1}(2)$	0.8630*** (0.1095)	$\Psi_{1,1,1}(3)$	0.9455*** (0.0899)		
$\Psi_{1,1,3}(1)$	-0.0087 (0.0094)	$\Psi_{1,1,3}(2)$	-0.0341** (0.0169)	$\Psi_{1,1,3}(3)$	-0.0387*** (0.0118)		
$\Psi_{1,2,2}(1)$	1.4668*** (0.0847)	$\Psi_{1,2,2}(2)$	1.5761*** (0.1083)	$\Psi_{1,2,2}(3)$	1.0984*** (0.1030)		
$\Psi_{1,2,3}(1)$	0.0101** (0.0050)	$\Psi_{1,2,3}(2)$	-0.0041 (0.0090)	$\Psi_{1,2,3}(3)$	0.0054*** (0.0011)		
$\Psi_{1,3,2}(1)$	4.3751*** (1.0807)	$\Psi_{1,3,2}(2)$	1.9444* (1.0943)	$\Psi_{1,3,2}(3)$	2.4483* (1.3496)		
$\Psi_{1,3,3}(1)$	0.5884*** (0.0683)	$\Psi_{1,3,3}(2)$	0.4538*** (0.0955)	$\Psi_{1,3,3}(3)$	1.3219*** (0.1167)		
$\Omega_{1,1}(1)$	0.0813*** (0.0034)	$\Omega_{1,1}(2)$	0.0747*** (0.0048)	$\Omega_{1,1}(3)$	0.0844*** (0.0041)		
$\Omega_{2,1}(1)$	-0.0056** (0.0025)	$\Omega_{2,1}(2)$	-0.0045 (0.0042)	$\Omega_{2,1}(3)$	-0.0116*** (0.0039)		
$\Omega_{2,2}(1)$	0.0394*** (0.0014)	$\Omega_{2,2}(2)$	0.0408*** (0.0023)	$\Omega_{2,2}(3)$	0.0522*** (0.0028)		
$\Omega_{3,1}(1)$	-0.0907** (0.0384)	$\Omega_{3,1}(2)$	-0.0198 (0.0381)	$\Omega_{3,1}(3)$	-0.1107** (0.0446)		
$\Omega_{3,2}(1)$	0.1800** (0.0350)	$\Omega_{3,2}(2)$	0.1070*** (0.0393)	$\Omega_{3,2}(3)$	0.3772*** (0.0407)		
$\Omega_{3,3}(1)$	0.5732*** (0.0217)	$\Omega_{3,3}(2)$	0.3904*** (0.0312)	$\Omega_{3,3}(3)$	0.5131*** (0.0264)		
$v(1)$	3.3412*** (0.2095)	$v(2)$	3.3006*** (0.3037)	$v(3)$	3.1541*** (0.2392)		

Note: $C_1 < 1$ is covariance stationarity of regime 1; $C_2 < 1$ is covariance stationarity of regime 2; $C_3 < 1$ is covariance stationarity of regime 3. The Ljung-Box (LB) statistics (p -values in parentheses) use the lag-order $\sqrt{T} \approx 28$. Log-likelihood (LL); Akaike information criterion (AIC); Bayesian information criterion (BIC); Hannan-Quinn criterion (HQC). Gradient-based standard errors are reported in parentheses.

*Parameter significance at the 15% level.

**Parameter significance at the 10% level.

***Parameter significance at the 5% level.

****Parameter significance at the 1% level.

than us for the last 250 years period, and therefore could separate the future climate impacts of humanity from the long-run effects of exogenous orbital variables.

CRedit authorship contribution statement

Szabolcs Blazsek: Conceptualization, Methodology, Software, Validation, Writing. **Alvaro Escribano:** Conceptualization, Methodology, Validation, Writing, Resources.

Declaration of competing interest

The authors declare that they have no known competing financial interests or personal relationships that could have appeared to influence the work reported in this paper.

Acknowledgments

The authors are thankful for the comments and suggestions of the associate editor and referees of the journal, Istvan Blazsek, Jennifer Castle, Matthew Copley, David Hendry, and Eric Hillebrand. This paper was presented at the Hungarian Economic Society Annual Conference (Budapest, December 2022). The comments and suggestions of conference participants and discussion of Erzsebet Kristof are greatly

appreciated. All remaining errors are our own. Computer codes are available from the authors of this paper upon request. Blazsek acknowledges funding from Universidad Francisco Marroquín, Guatemala. Escribano acknowledges funding from Ministerio de Economía, Industria y Competitividad, Spain (ECO2016-00105-001 and MDM 2014-0431), Comunidad de Madrid, Spain (MadEco-CM S2015/HUM-3444), and Agencia Estatal de Investigación, Spain (2019/00419/001). The authors declare no conflict of interest. The material in this article does not reflect the positions of any of the institutions to which the authors are affiliated.

Appendix A

See Tables A.1–A.3.

Appendix B. Supplementary data

Supplementary material related to this article can be found online at <https://doi.org/10.1016/j.eneco.2023.106522>.

References

Ayala, A., Blazsek, S., Escribano, A., 2022. Anticipating extreme losses using score-driven shape filters. Stud. Nonlinear Dyn. Econ. <http://dx.doi.org/10.1515/snde-2021-0102>.

- Blasques, F., van Brummelen, J., Koopman, S.J., Lucas, A., 2022. Maximum likelihood estimation for score-driven models. *J. Econometrics* 227 (2), 325–346. <http://dx.doi.org/10.1016/j.jeconom.2021.06.003>.
- Blasques, F., Koopman, S.J., Lucas, A., 2015. Information-theoretic optimality of observation-driven time series models for continuous responses. *Biometrika* 102 (2), 325–343. <http://dx.doi.org/10.1093/biomet/asu076>.
- Blazsek, S., Escribano, A., 2016a. Patent propensity, R & D and market competition: Dynamic spillovers of innovation leaders and followers. *J. Econometrics* 191 (1), 145–163. <http://dx.doi.org/10.1016/j.jeconom.2015.10.005>.
- Blazsek, S., Escribano, A., 2016b. Score-driven dynamic patent count panel data models. *Econom. Lett.* 149 (C), 116–119. <http://dx.doi.org/10.1016/j.econlet.2016.10.026>.
- Blazsek, S., Escribano, A., 2022. Robust estimation and forecasting of climate change using score-driven ice-age models. *Econom. (Special Issue: Econom. Anal. Clim. Change)* 10 (1), <http://dx.doi.org/10.3390/econometrics10010009>.
- Blazsek, S., Escribano, A., Licht, A., 2021. Multivariate Markov-switching score-driven models: An application to the global crude oil market. *Stud. Nonlinear Dyn. Econ.* <http://dx.doi.org/10.1515/snede-2020-0099>.
- Blazsek, S., Escribano, A., Licht, A., 2022a. Co-integration with score-driven models: an application to US real GDP growth, US inflation rate, and effective federal funds rate. *Macroecon. Dyn.* <http://dx.doi.org/10.1017/S1365100521000365>.
- Blazsek, S., Escribano, A., Licht, A., 2022b. Score-driven location plus scale models: Asymptotic theory and an application to forecasting Dow Jones volatility. *Stud. Nonlinear Dyn. Econ.* <http://dx.doi.org/10.1515/snede-2021-0083>.
- Bollerslev, T., 1986. Generalized autoregressive conditional heteroskedasticity. *J. Econometrics* 31 (3), 307–327. [http://dx.doi.org/10.1016/0304-4076\(86\)90063-1](http://dx.doi.org/10.1016/0304-4076(86)90063-1).
- Box, G.E.P., Jenkins, G.M., 1970. *Time Series Analysis, Forecasting and Control*. Holden-Day, San Francisco, US.
- Castle, J., Hendry, D.F., 2020. Climate econometrics: An overview. *Found. Trends Econom.* 10 (3–4), 145–322. <http://dx.doi.org/10.1561/08000000037>.
- Cox, D.R., 1981. Statistical analysis of time series: Some recent developments. *Scand. J. Stat.* 8 (2), 93–115. <https://www.jstor.org/stable/i412423>.
- Creal, D., Koopman, S.J., Lucas, A., 2008. A general framework for observation driven time-varying parameter models. In: Tinbergen Institute Discussion Paper 08-108/4. <https://papers.tinbergen.nl/08108.pdf>.
- Engle, R.F., 1982. Autoregressive conditional heteroscedasticity with estimates of the variance of United Kingdom inflation. *Econometrica* 50 (4), 987–1007. <http://dx.doi.org/10.2307/1912773>.
- Everitt, B.S., 1993. *Cluster Analysis*, third ed. Halsted Press, London, UK, New York, US.
- Harvey, A.C., 2013. *Dynamic Models for Volatility and Heavy Tails: With Applications to Financial and Economic Time Series*. In: *Econometric Society Monographs*, Cambridge University Press, Cambridge, UK.
- Harvey, A.C., Chakravarty, T., 2008. Beta-t(e)garch. In: *Cambridge Working Papers in Economics* 0840, Faculty of Economics. University of Cambridge, Cambridge, <https://www.repository.cam.ac.uk/handle/1810/229418>.
- Intergovernmental Panel on Climate Change, 2021. Sixth assessment report. <https://www.ipcc.ch/report/ar6/wg1/#SPM>.
- Jouzel, J., Masson-Delmotte, V., Cattani, O., Dreyfus, G., Falourd, S., Hoffmann, G.E., 2007. Orbital and millennial antarctic climate variability over the past 800, 000 years. *Science* 317, 793–797. <http://dx.doi.org/10.1126/science.1141038>.
- Kasahara, H., Shimotsu, K., 2018. Testing the number of regimes in Markov regime switching models. <https://arxiv.org/pdf/1801.06862.pdf>.
- Lisiecki, L.E., Raymo, M.E., 2005. A pliocene-pleistocene stack of 57 globally distributed benthic $\delta^{18}\text{O}$ records. *Paleoceanography* 20 (1), <http://dx.doi.org/10.1029/2004PA001071>.
- Ljung, G.M., Box, G.E.P., 1978. On a measure of lack of fit in time-series models. *Biometrika* 65 (2), 297–303. <http://dx.doi.org/10.1093/biomet/65.2.297>.
- Lüthi, D., Le Floch, M., Bereiter, B., Blunier, T., Barnola, J.-M., Steigenthaler, U., Raynaud, D., Jouzel, J., Fischer, H., Kawamura, K., Stocker, T.F., 2008. High-resolution carbon dioxide concentration record 650, 000–800, 000 years before present. *Nature* 453, <http://dx.doi.org/10.1038/nature06949>.
- Paillard, D., Labeyrie, L.D., Yiou, P., 1996. Macintosh program performs time-series analysis. *Eos Trans. AGU* 77 (39), 379. <http://dx.doi.org/10.1029/96EO00259>.
- Ruddiman, W., 2005. *Plows, Plagues and Petroleum: How Humans Took Control of the Climate*. Princeton University Press, Princeton, US.
- Tiao, G.C., Tsay, R.S., 1989. Model specification in multivariate time series. *J. R. Stat. Soc.* 51 (2), 157–213. <http://dx.doi.org/10.1111/j.2517-6161.1989.tb01756.x>.
- Ward, J.H., 1963. Hierarchical grouping to optimize an objective function. *J. Amer. Statist. Assoc.* 58 (301), 236–244. <http://dx.doi.org/10.1080/01621459.1963.10500845>.